FFI RAPPORT

Microscopic studies of wolfram carbide after fracturing

Frøyland Øyvind, Moxnes John F

FFI/RAPPORT-2004/01883

FFI-V/860/01

Approved
Kjeller 2004-02-23

Bjarne Haugstad
Director of Research

Microscopic studies of wolfram carbide after fracturing

Frøyland Øyvind, Moxnes John F

FFI/RAPPORT-2004/01883

FORSVARETS FORSKNINGSINSTITUTT
Norwegian Defence Research Establishment
P O Box 25, NO-2027 Kjeller, Norway

FORSVARETS FORSKNINGSINSTITUTT (FFI)
Norwegian Defence Research Establishment

P O BOX 25
N0-2027 KJELLER, NORWAY

UNCLASSIFIED

SECURITY CLASSIFICATION OF THIS PAGE (when data entered)

REPORT DOCUMENTATION PAGE

1) PUBL/REPORT NUMBER	2) SECURITY CLASSIFICATION	3) NUMBER OF PAGES
FFI/RAPPORT-2004/1883	UNCLASSIFIED	36
1a) PROJECT REFERENCE	**2a) DECLASSIFICATION/DOWNGRADING SCHEDULE**	
FFI-V/860/01	-	

4) TITLE

Microscopic studies of wolfram carbide after fracturing

5) NAMES OF AUTHOR(S) IN FULL (surname first)

Frøyland Øyvind, Moxnes John F

6) DISTRIBUTION STATEMENT

Approved for public release. Distribution unlimited. (Offentlig tilgjengelig)

2004) **INDEXING TERMS**

IN ENGLISH:	IN NORWEGIAN:
a) Crack	a) Sprekk
b) SEM	b) SEM
c) Microscopy	c) Mikroskopi
d) Wolfram Carbide	d) Wolfram karbid
e) Penetrator	e) Penetrator

THESAURUS REFERENCE:

8) ABSTRACT

In this report a study of the microscopic properties of a fractured sintered wolfram carbide-cobalt penetrator has been carried out. Scanning electron microscopy (SEM) and light microscopy are used to study the fracture mechanics of the WC-Co hardmetal during different loading conditions.

We found that the crack path is mainly intergranular along the WC-Co boundaries both under static and dynamic loadings. Crack paths across the WC phase, namely transgranular, were seen clearly in a few cases for cracks emanating from indentations made with a Vickers hardness tester. Also the analyses highlights some defects that can be present when processing conditions have been suboptimal.

9) DATE	AUTHORIZED BY This page only	POSITION
2004-02-23	Bjarne Haugstad	Director of Research

ISBN 82-464-0921-2

UNCLASSIFIED

SECURITY CLASSIFICATION OF THIS PAGE (when data entered)

CONTENTS

Microscopic studies of wolfram carbide after fracturing

1 INTRODUCTION

Nammo Raufoss AS is the inventor of the Multipurpose (MP) ammunition concept. The MP technology was developed during the end of the 60s and the first series production started in the beginning of the 70s. Still the product is of great importance for the company's medium calibre division. Large volumes of ammunition are delivered for the armed forces around the world and in Norway.

The hard core of the 12.7 mm MP projectile consists of a high-density Wolfram Carbide-Cobalt (WC-Co) hardmetal. The penetration capabilities of the hard core are of course strongly dependent of the material properties. The tensile and compressive strength of this ceramic is very attractive. The greatest limitation in using ceramic materials is the in general low ductility in comparison to for instance steel material. Thus when the stresses reaches the fracture surface the low ductility leads to a fast decrease in the strength due to damage. For steel materials the strength stays high for much larger plastic strains.

In an earlier study, the following macroscopic test have been carried out on the WC-Co [1], i) a bending test of the hardcore to establish the tensile strength, ii) a compression test to establish the compressive strength, iii) a shooting test of inert 12.7 mm projectiles at the firing range in order to study fragmentation pattern after penetration, iv) a static firing test by use of a "squib" in order to study the hard core fragments and finally v) a shooting test at the firing range with 12.7 mm MP projectiles. The five tests could in principle give different kinds of fracture mechanisms of the hardcore. Our main object in this report is simply to study the different fracture surfaces microscopically. By doing this we can hopefully establish whether the static tests give the same type of fracturing as more dynamic tests. This is important knowledge for any physical based fracture model.

Different types of fracture that can be achieved:

- intergranular fracture
- transgranular fracture

During intergranular fracture growth it is also important to establish whether the Cobalt, which acts as a binder, is fractured at the boundary of the WC, or whether the Cobalt fractures in the pure Cobalt phase.

The WC-Co hardmetals are the product of a mature and reasonably well understood technology. Still the behaviour during high stresses and strain rates is poorly understood. Typically most ceramic materials as for instance WC-Co, are studied as of they were armour

plates. Our approach is different since our study is focused on use of the hardmetal as a penetrator. We believe that this approach will highlight some main characteristics more clearly than during use as an armour plate.

2 THE BENDING TEST

After bending during a three point bending test the WC-Co hardmetal fractured into two different pieces. Sandvik Hard Materials manufactured the WC-Co specimen. The fracture surface is shown in figure 2.1.

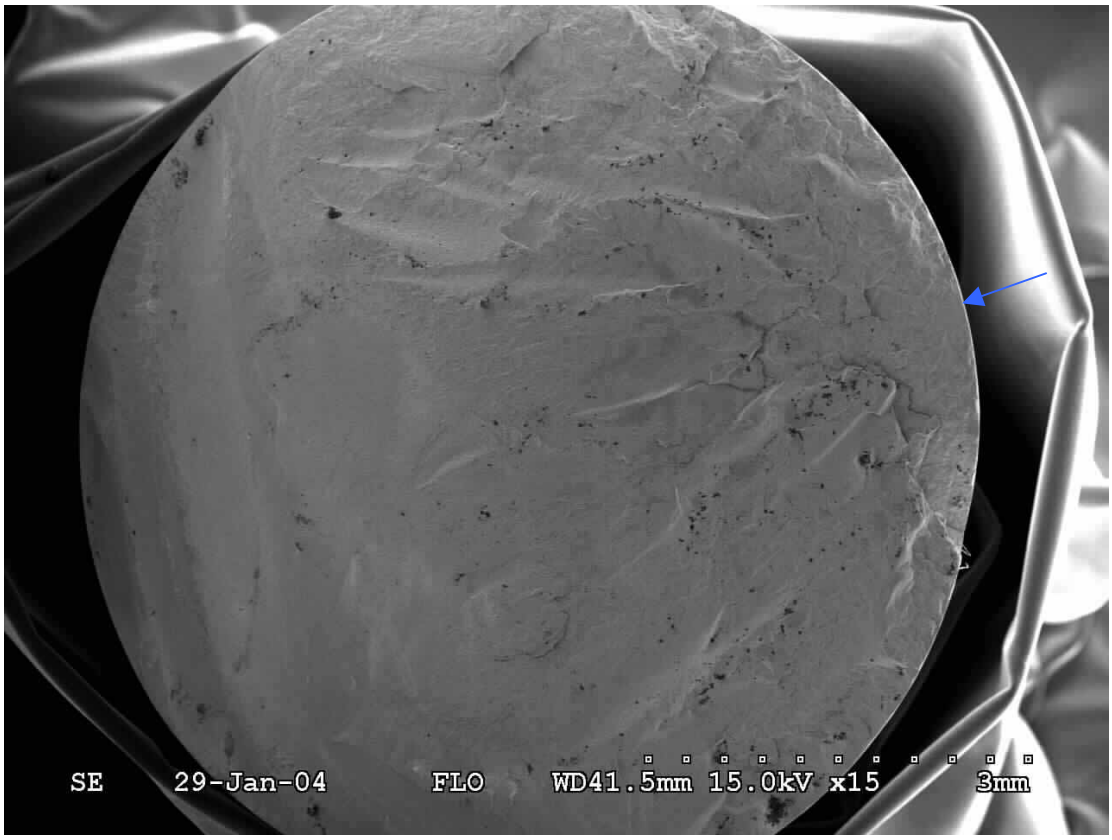

Figure 2.1: Overview of fracture surface.

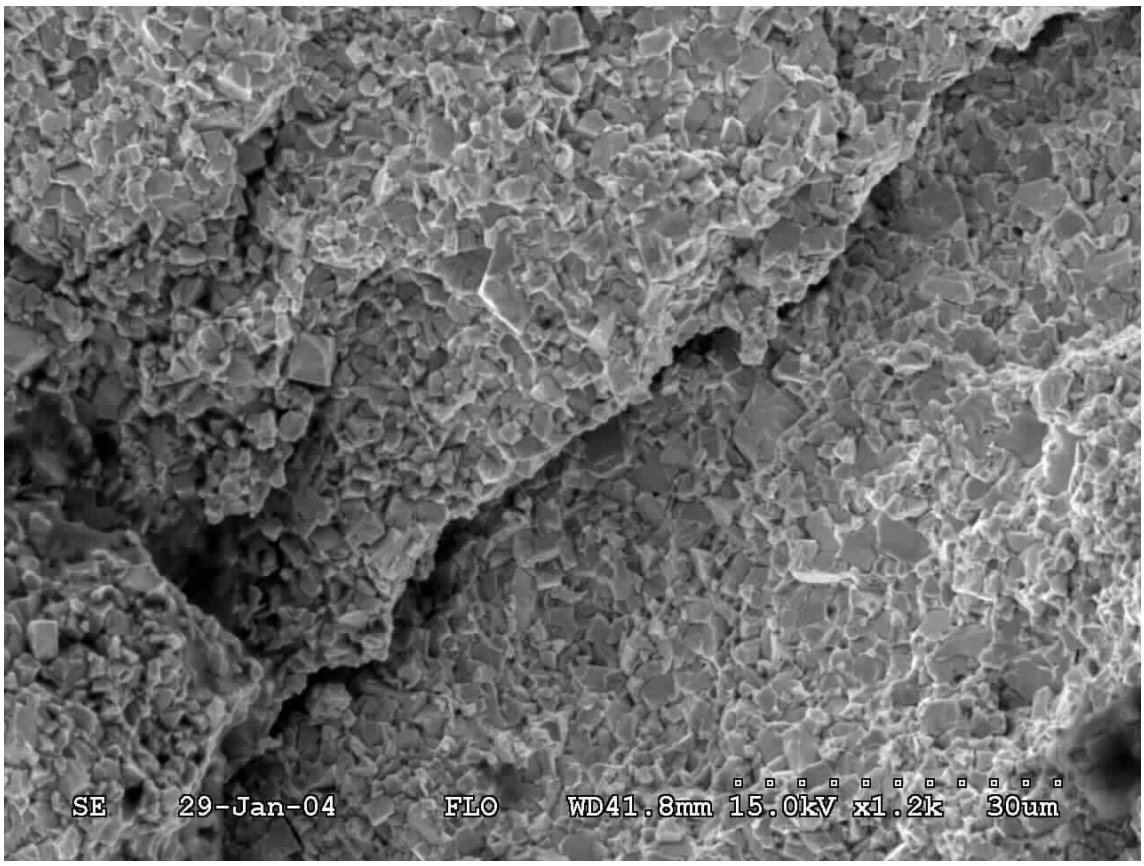

Figure 2.2: Fracture surface of WC-Co hardmetal in three point bending test.

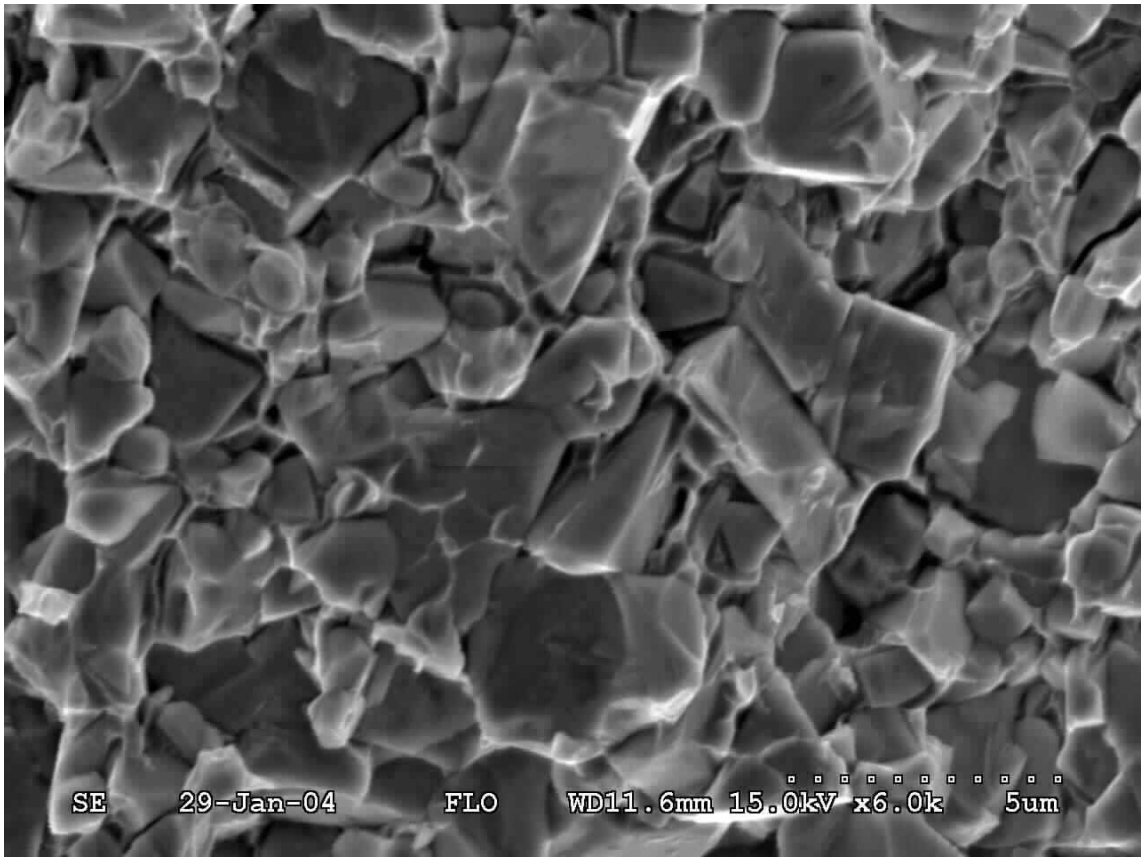

Figure 2.3: Fracture surface of WC-Co hardmetal in three point bending test.

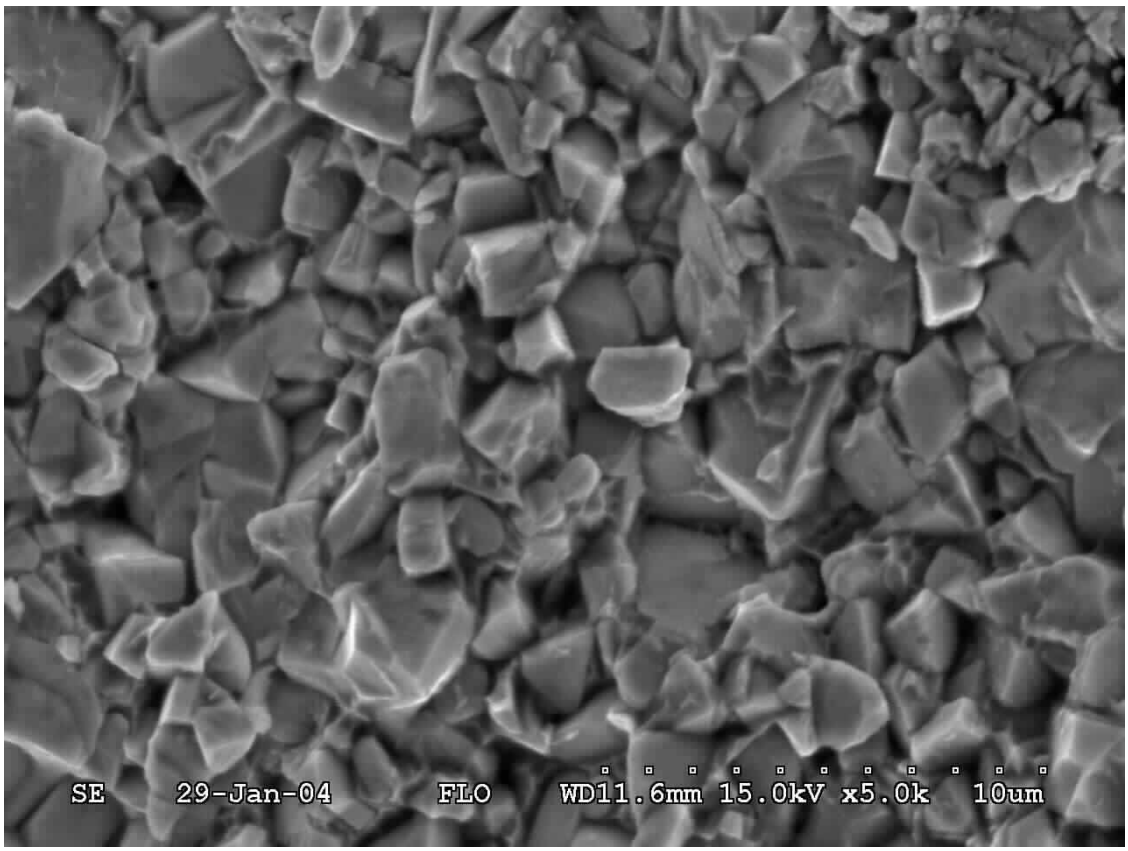

Figure 2.4: Fracture surface of WC-Co hardmetal in three point bending test.

We observe that the surface is microscopically rough with geometric grain shapes obvious. This identifies the fracture as intergranular. The arrow in figure 2.1 shows the origin of fracture.

3 THE COMPRESSION TEST

After compression in a simple compression test the hardcore fractured in many different pieces, and the fragments were collected for microscopic examination. The WC-Co hardmetals tested were made by two different manufacturers. The fracture surface is shown in figure 3.1

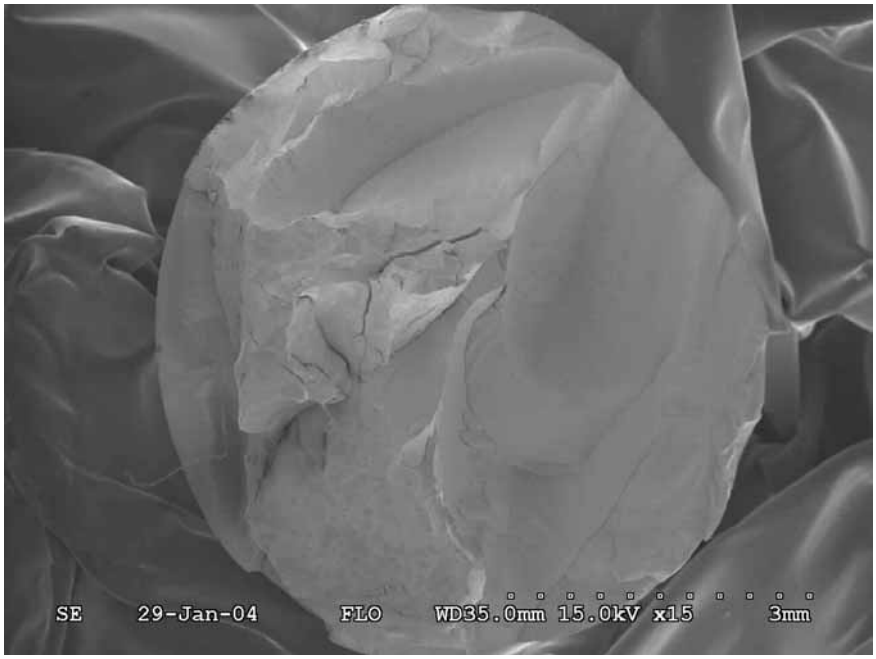

Figure 3.1: Overview of fracture surface (Sandvik Hard Materials)

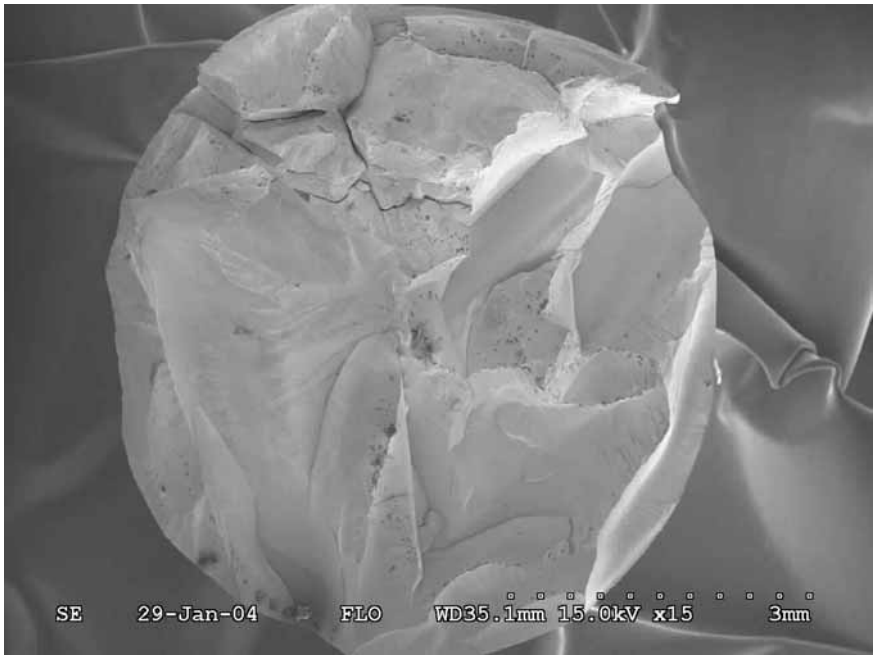

Figure3.2: Overview of fracture surface (Kennametal Hertel)

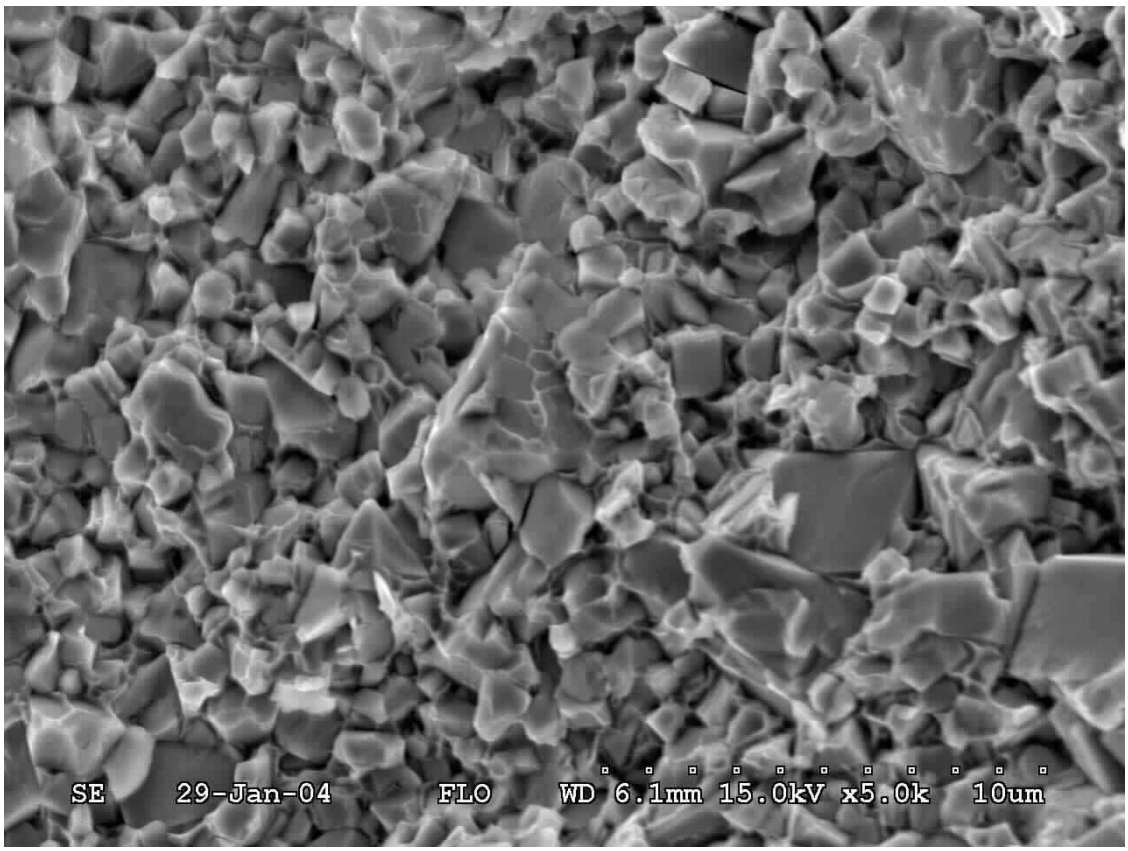

Figure 3.3: Fracture surface by compression. (Kennametal Hertel)

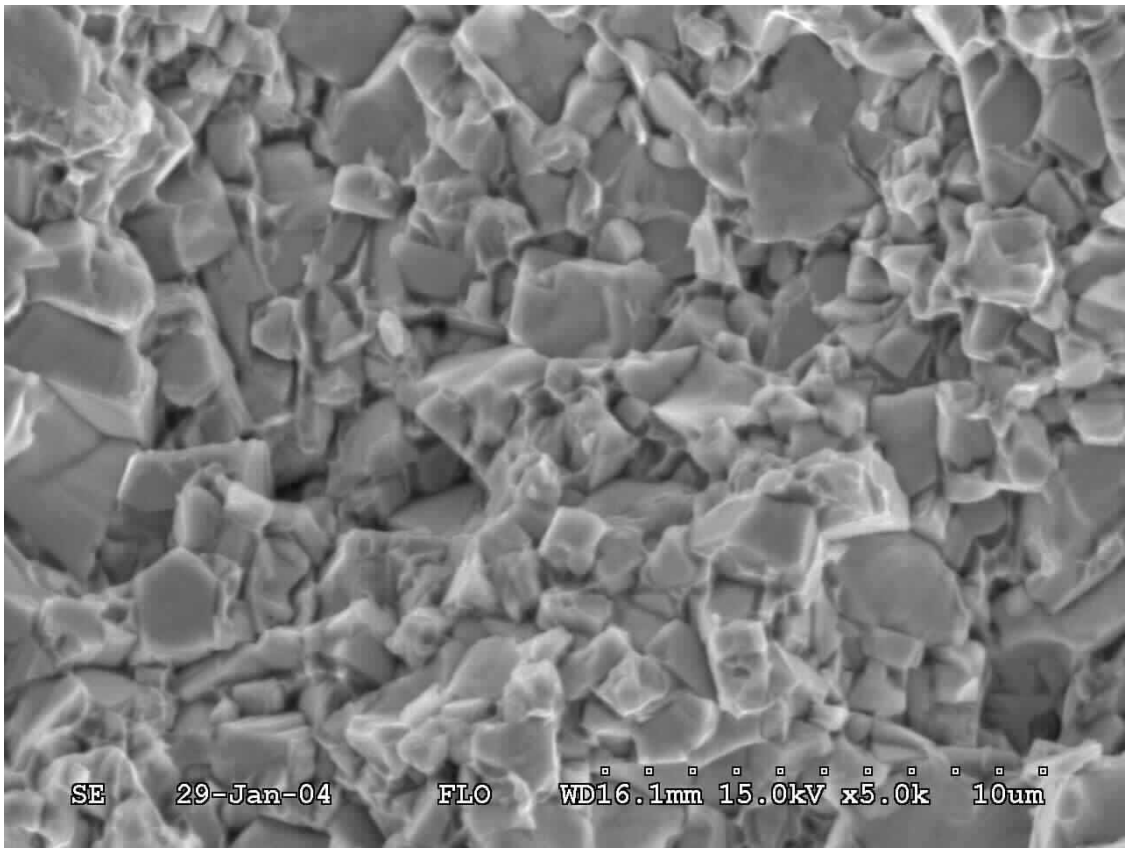

Figure 3.4: Fracture surface by compression. (Sandvik Hard Materials)

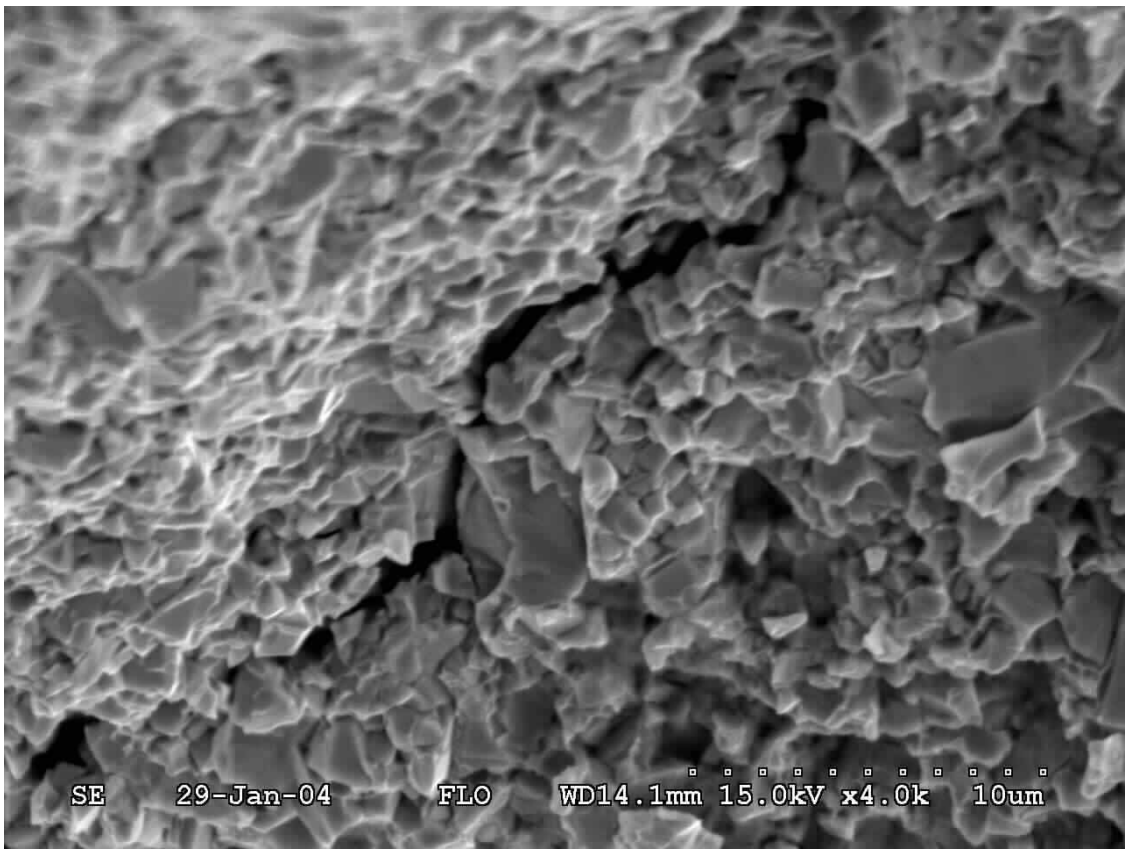

Figure 3.5: Fracture surface by compression with visible crack. (Kennametal Hertel)

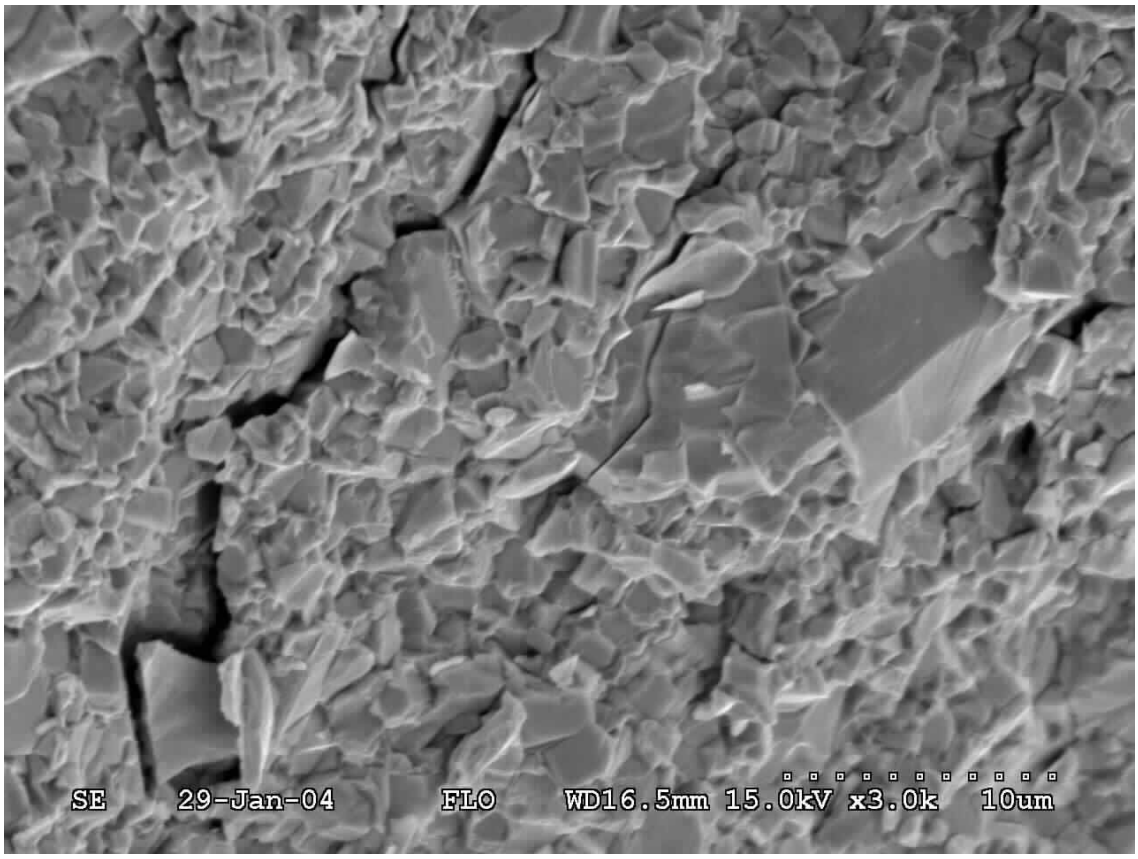

Figure 3.6: Fracture surface by compression with visible cracks. (Sandvik Hard Materials)

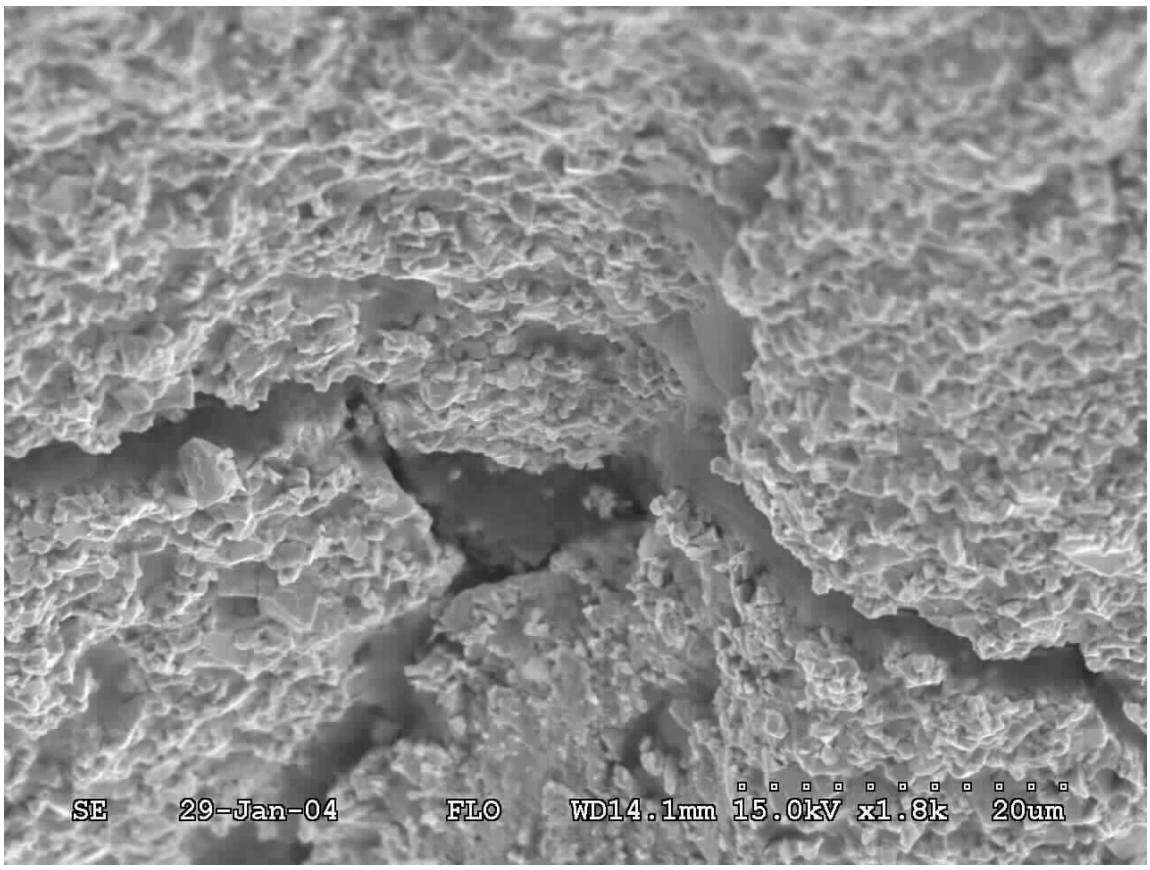

Figure 3.7: Fracture surface by compression with visible cracks. (Kennametal Hertel)

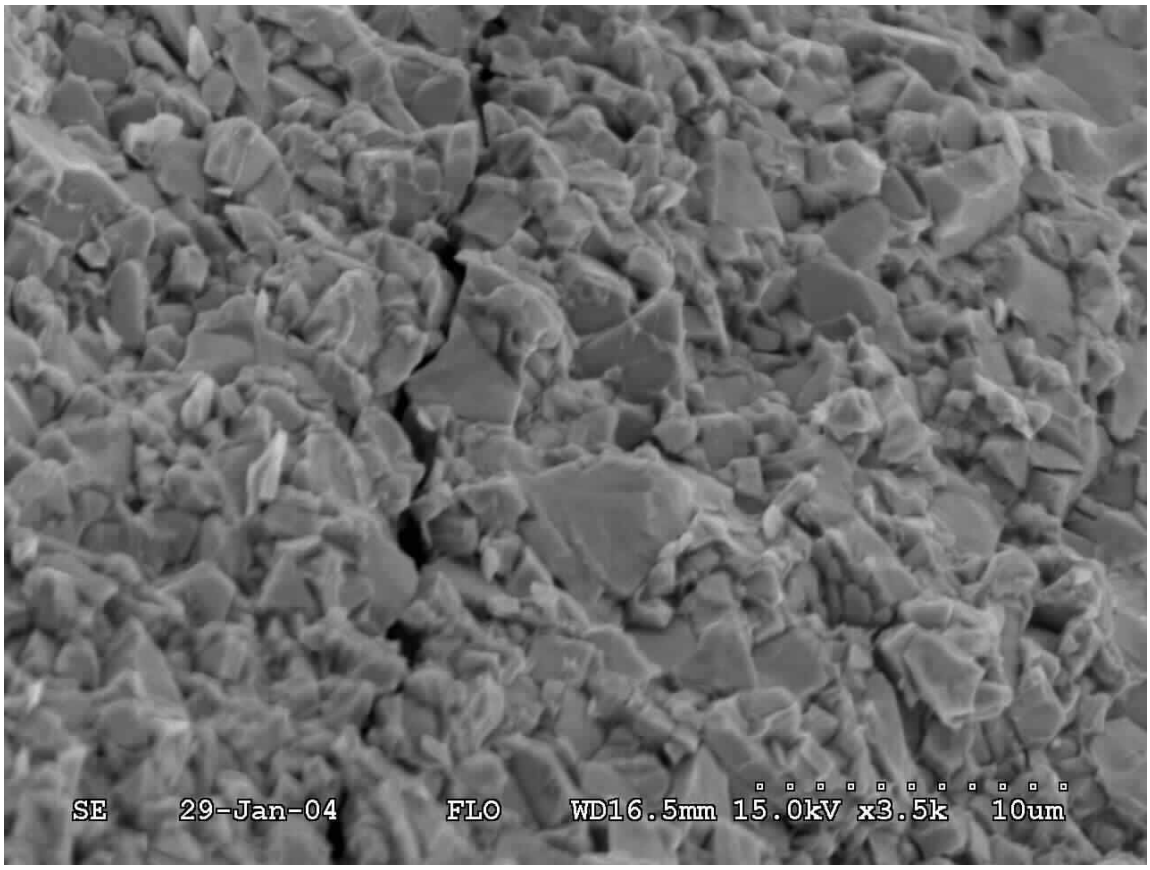

Figure 3.8: Fracture surface by compression with visible crack. (Sandvik Hard Materials)

We observe that the geometric shape of the WC grains are clearly visible. This indicates that the fracture is mainly intergranular. Also notice that the overall fracture surface is more

complex than for the bending test. This makes it difficult to point out a certain (maybe multiple) fracture origin.

4 SHOOTING TEST OF INERT PROJECTILES

The explosive in the hardcore was taken out and replaced with an inert ingredient. After firing through a 22 mm armour steel plate the fragments of the hard core were collected in a witness plate 36 cm behind the armour. Kennametal Hertel manufactures the WC-Co hardmetal.
The fracture surface is shown in figure 4.1.

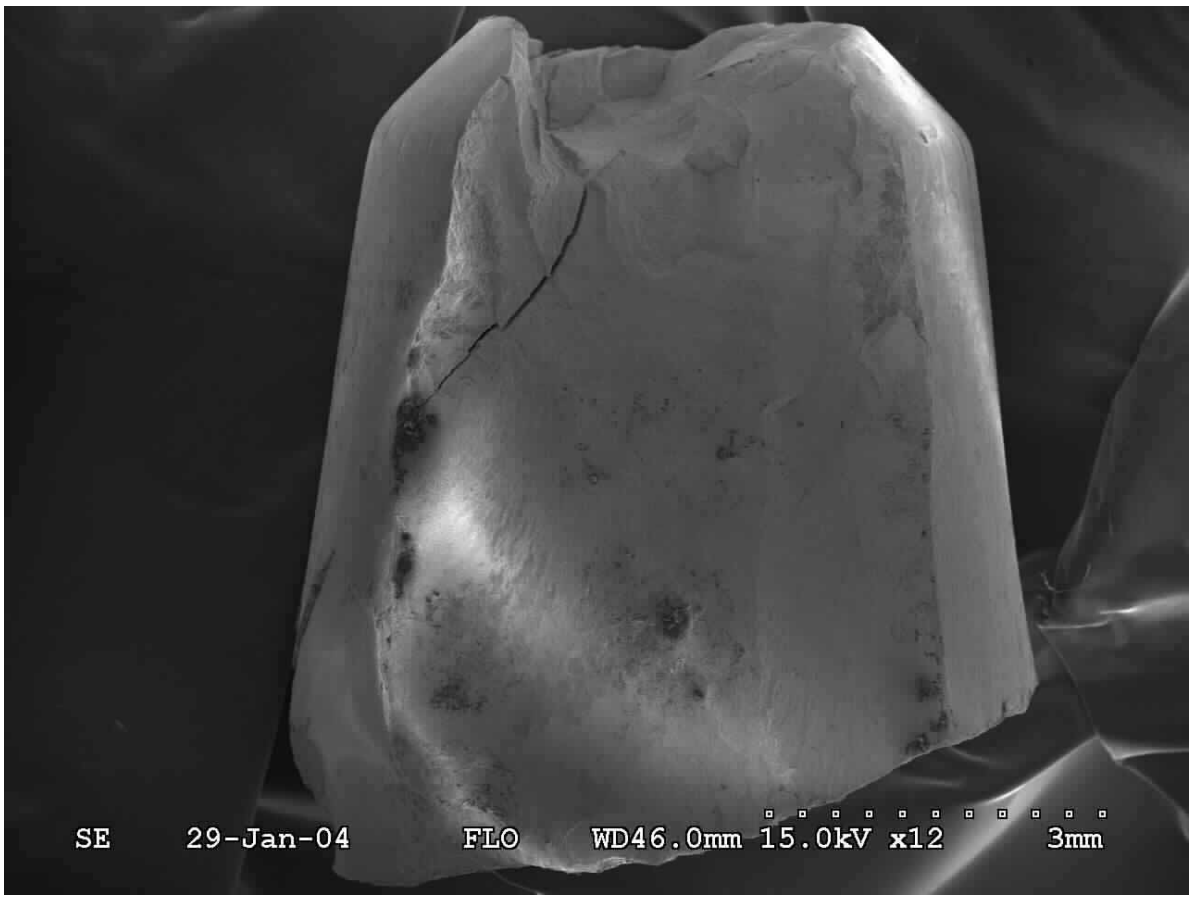

Figure 4.1: Overview of the fractured WC-Co specimen after shooting test into armour steel.

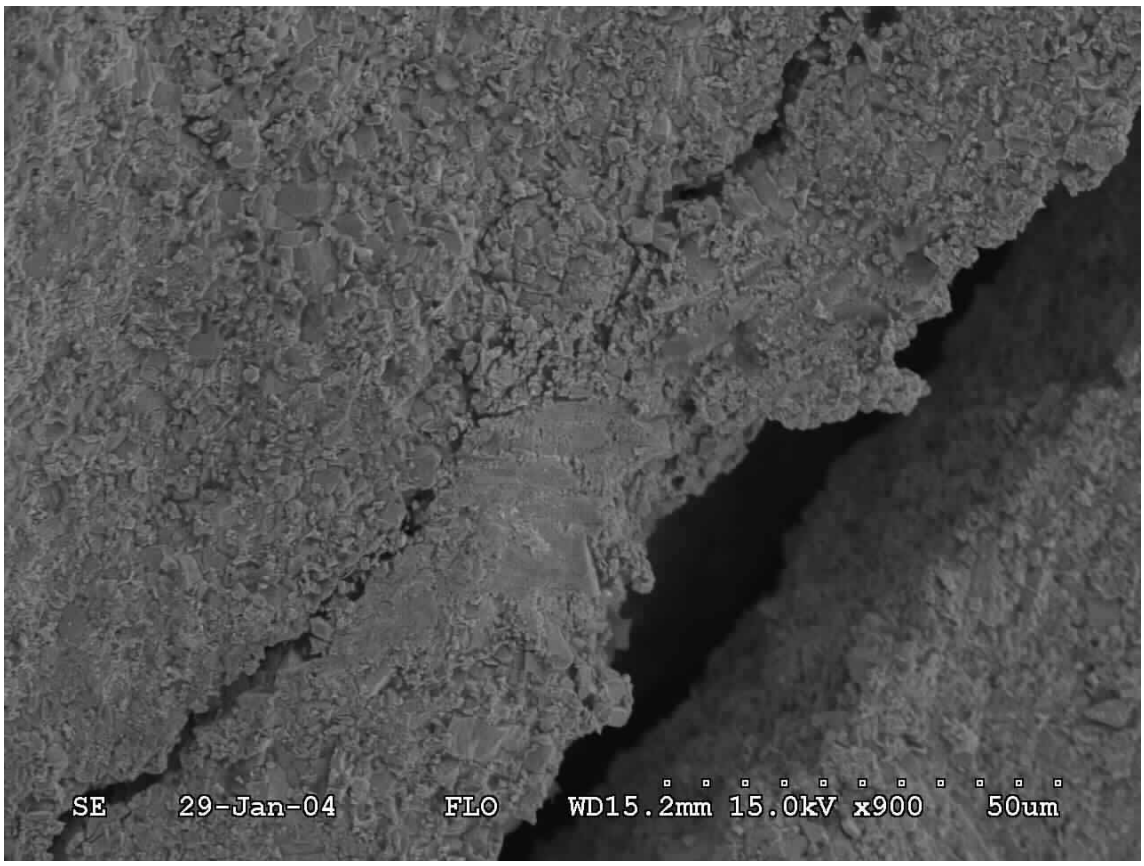

Figure 4.2: Fracture surface with cracks.

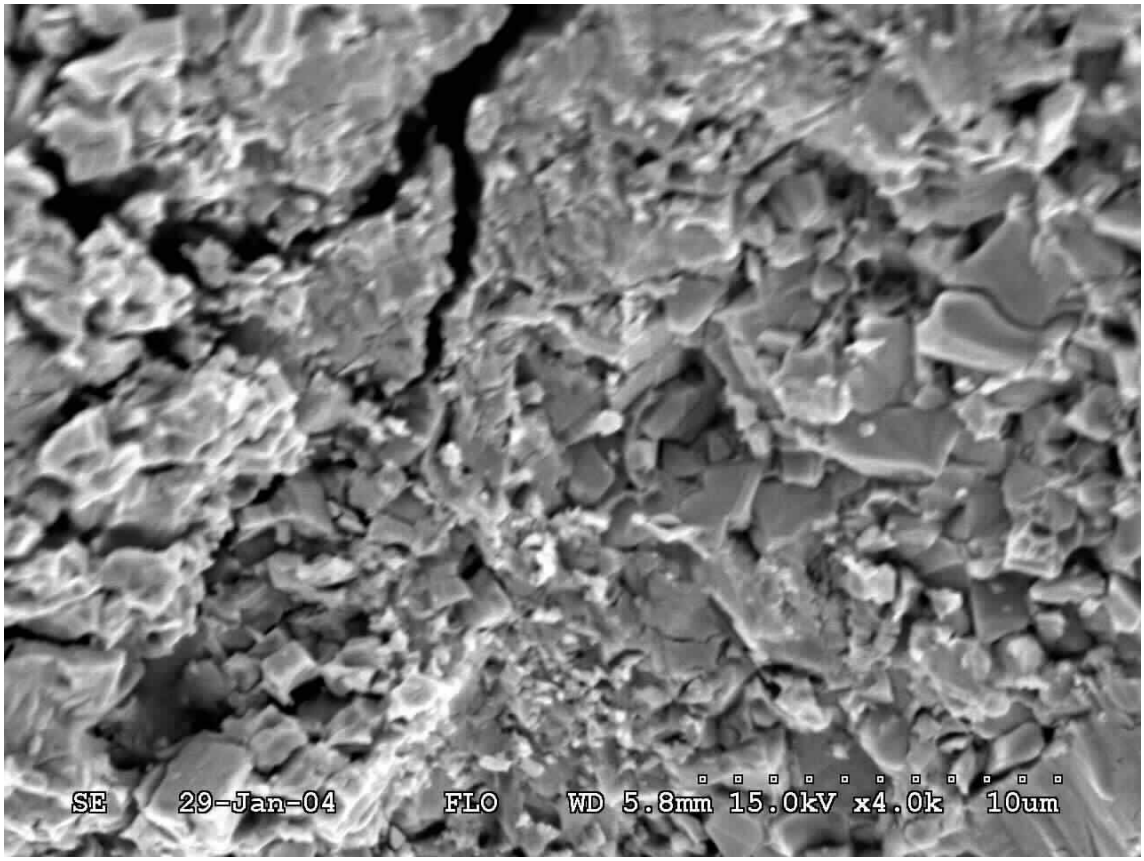

Figure 4.3: Fracture surface with cracks.

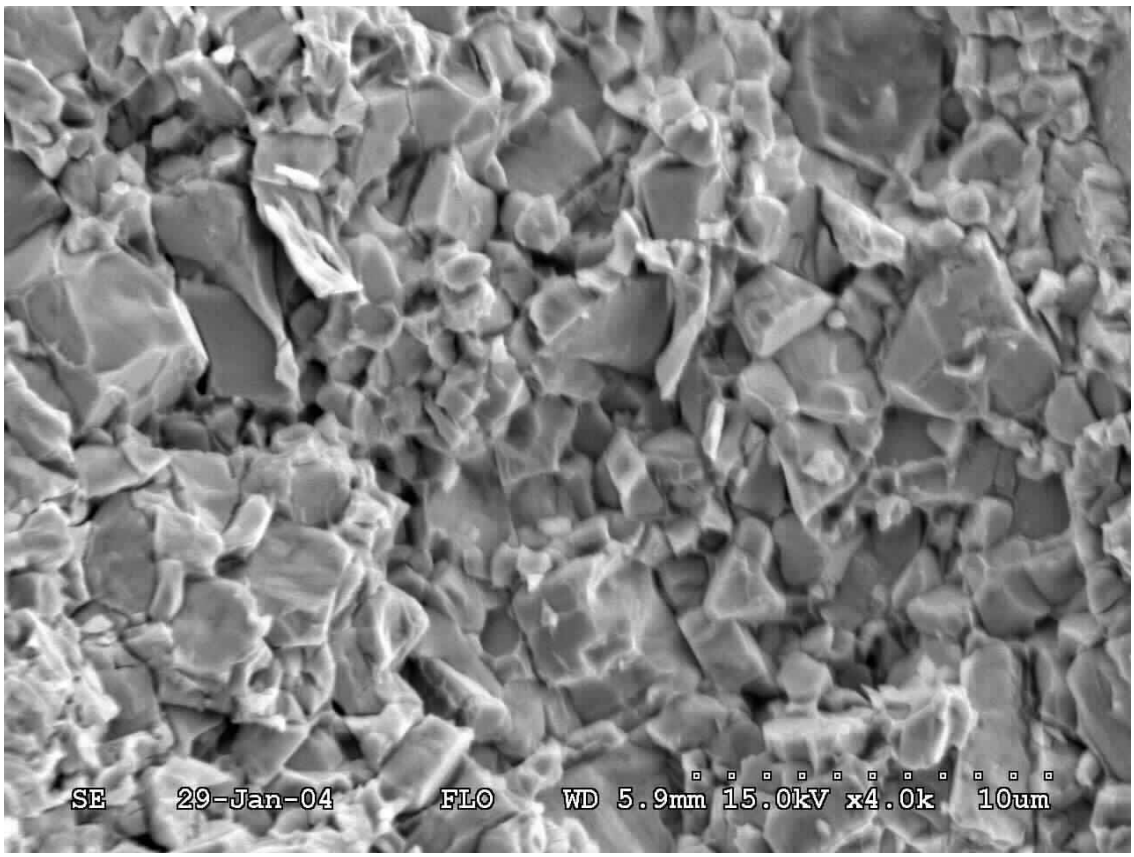

Figure 4.4: Microstructure of fracture surface.

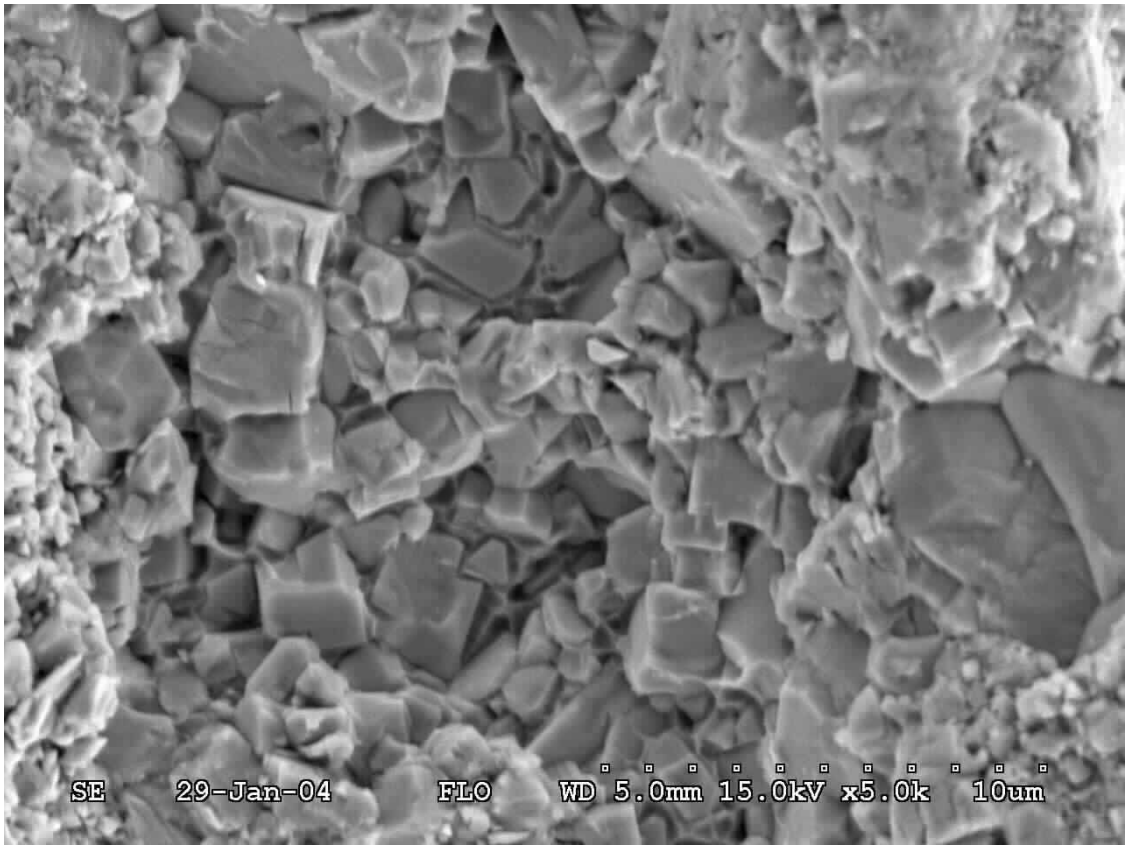

Figure 4.5: Microstructure of fracture surface.

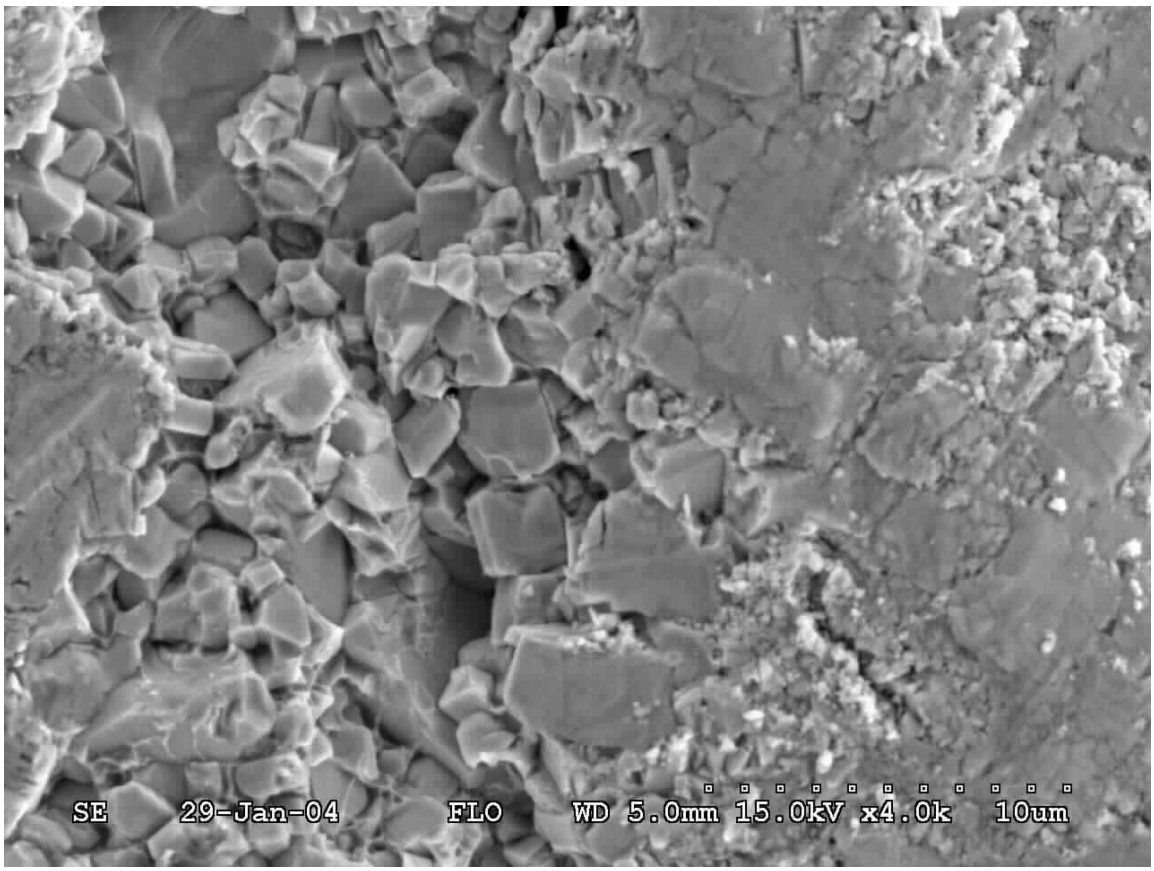

Figure 4.6: Microstructure of fracture surface.

Again the geometric shape of the WC grains are conspicuous, which indicates an intergranular fracture. The microstructure of the fracture surface seems to have suffered damage (fig. 4.6) from secondary impacts also.

5 STATIC IGNITION OF PROJECTILE

The explosive in the projectile was statically ignited with a squib (M100). The fractured hard-core is seen in figure 5.1. The hardmetal was examined in a scanning electron microscope. Figure 5.2 shows the fracture surface.

Figure 5.1: Projectile after ignition of explosive (H764).

Figure 5.2: Overview of fracture surface from the specimen to the right in figure 5.1.

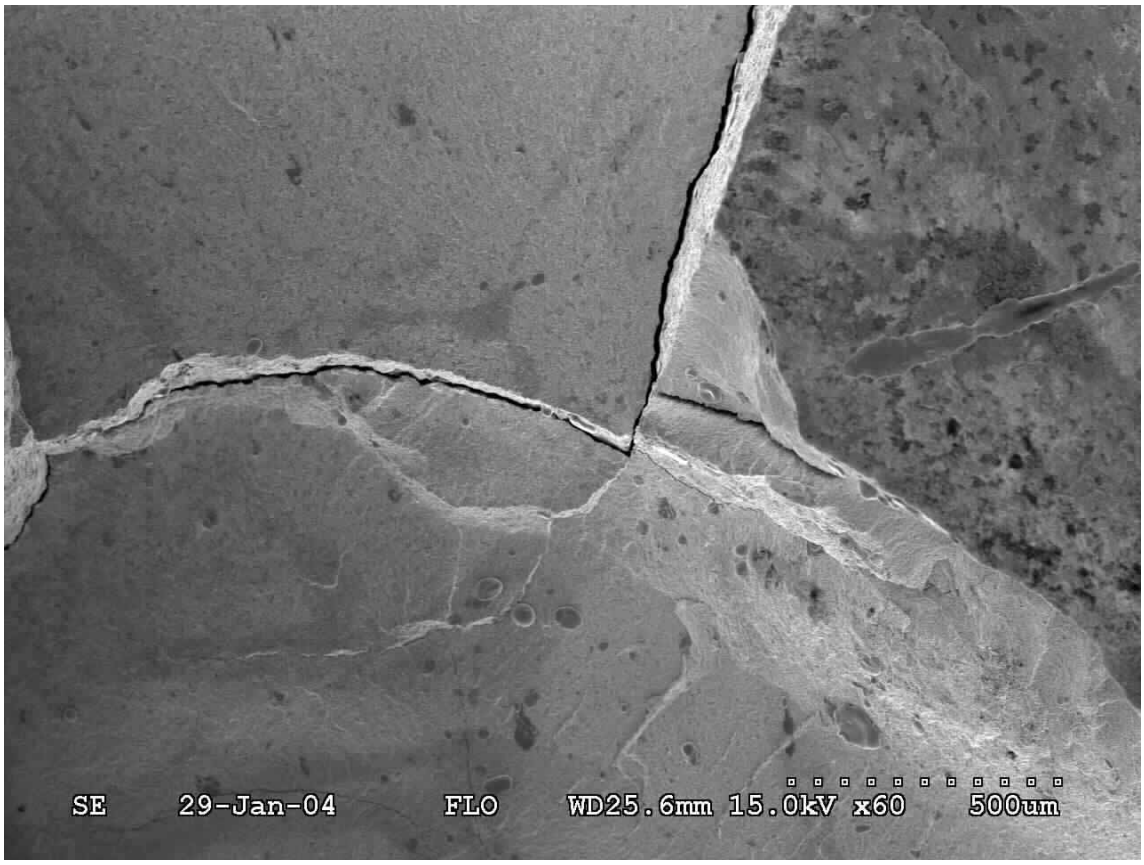

Figure 5.2: Fracture surface with cracks.

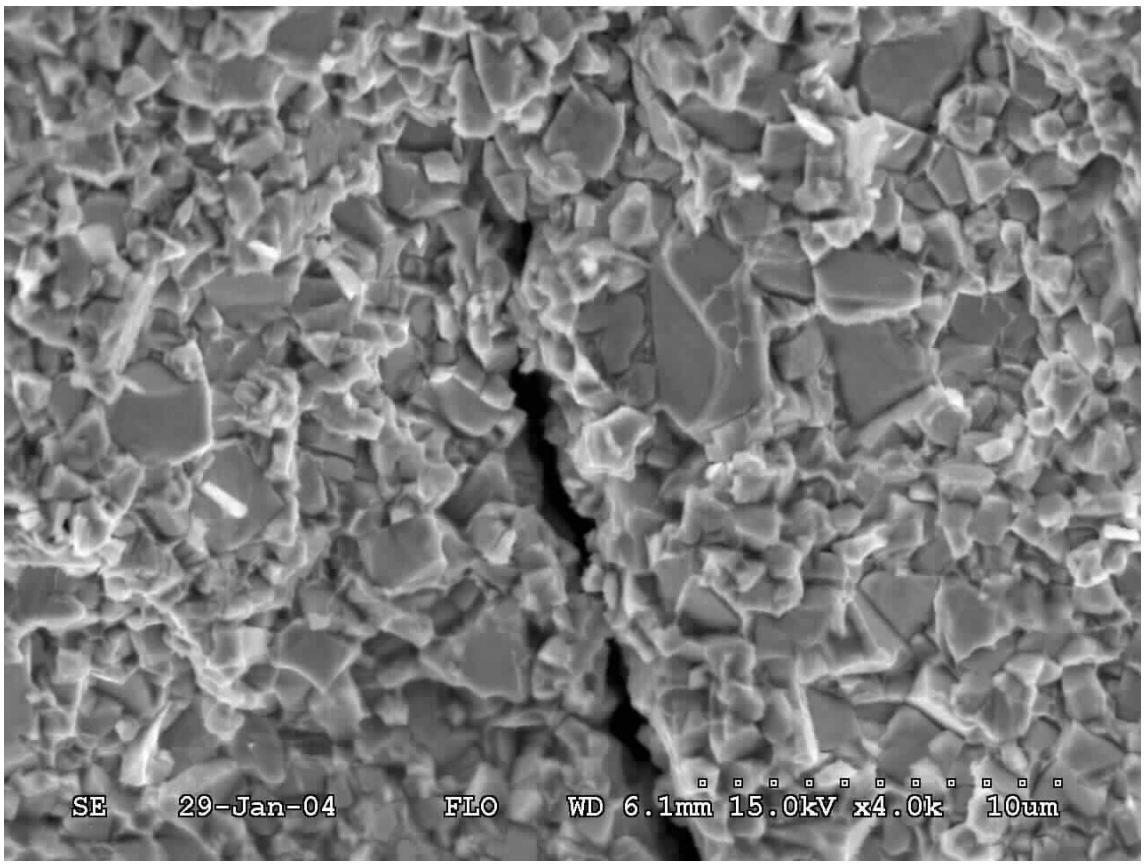

Figure 5.3: Fracture surface with crack.

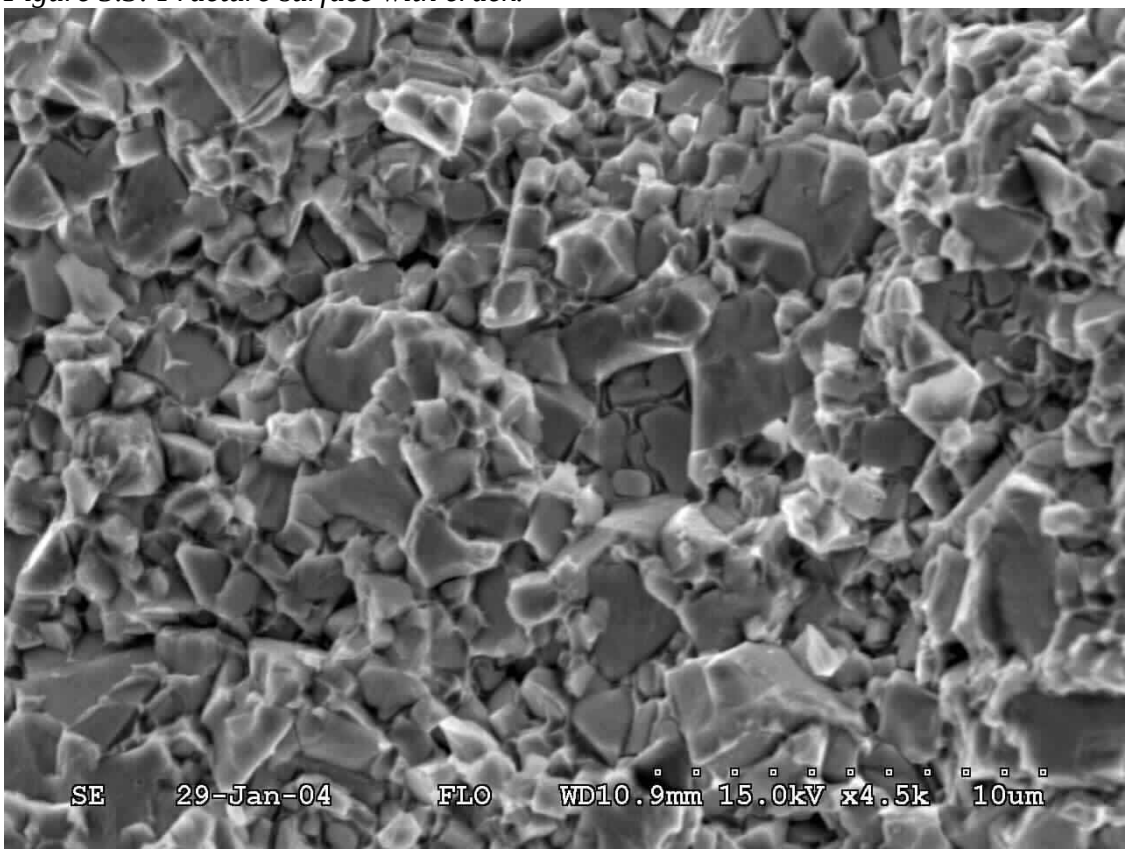

Figure 5.4: Fracture surface.

Again the fracture seems to be mainly intergranular. The fracture surface has also been contaminated with debris from the explosion.

6 LIVE FIRING EXPERIMENTS OF PROJECTILES

12.7 mm MP projectiles were fired at 22 mm armour steel plates at a distance of approximately 5 meters. Some of the fragments behind armour were examined microscopically. Figure 6.1 shows the fracture surface.

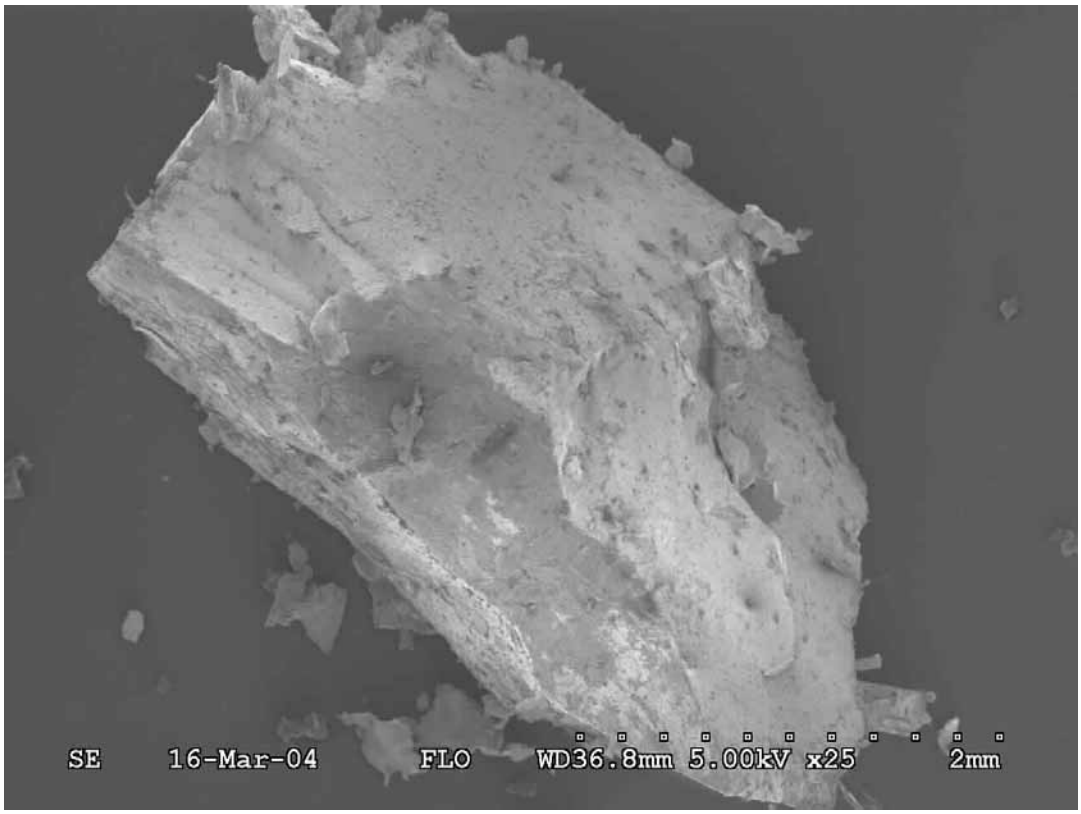

Figure 6.1:A piece of the fractured WC-Co hardmetal penetrator. (LOT …-00)

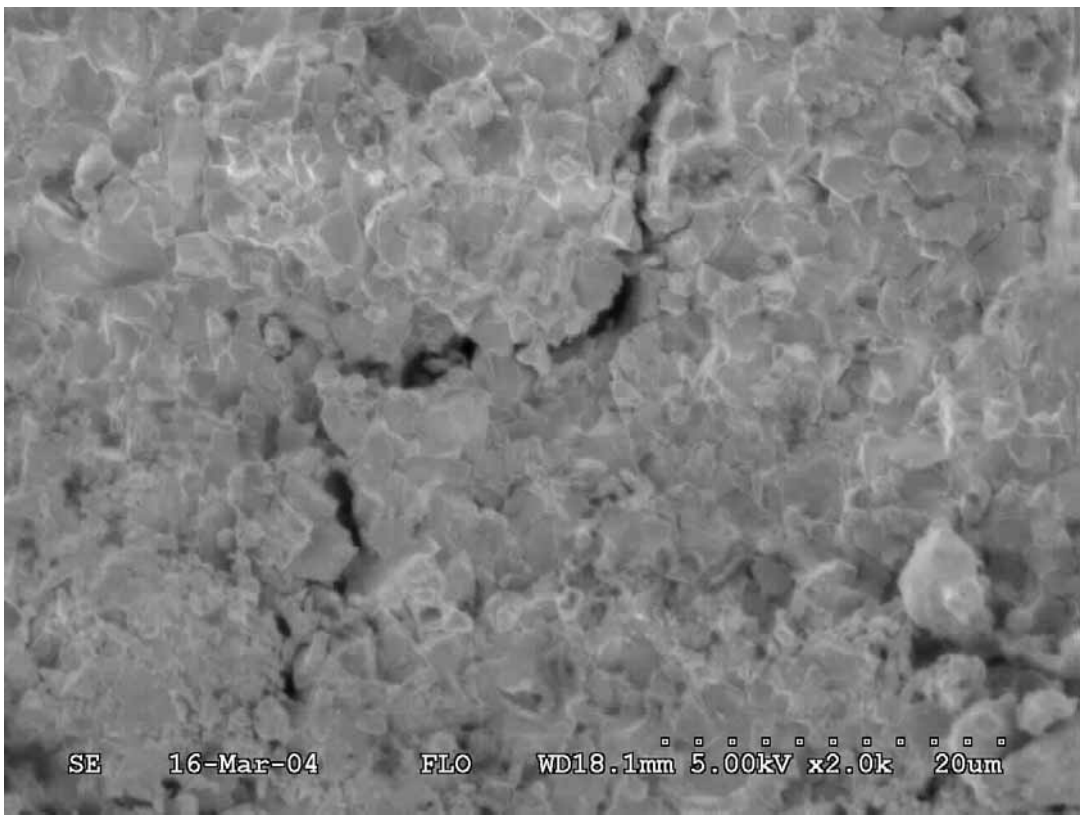

Figure 6.2: Fracture surface with crack. (LOT …-00)

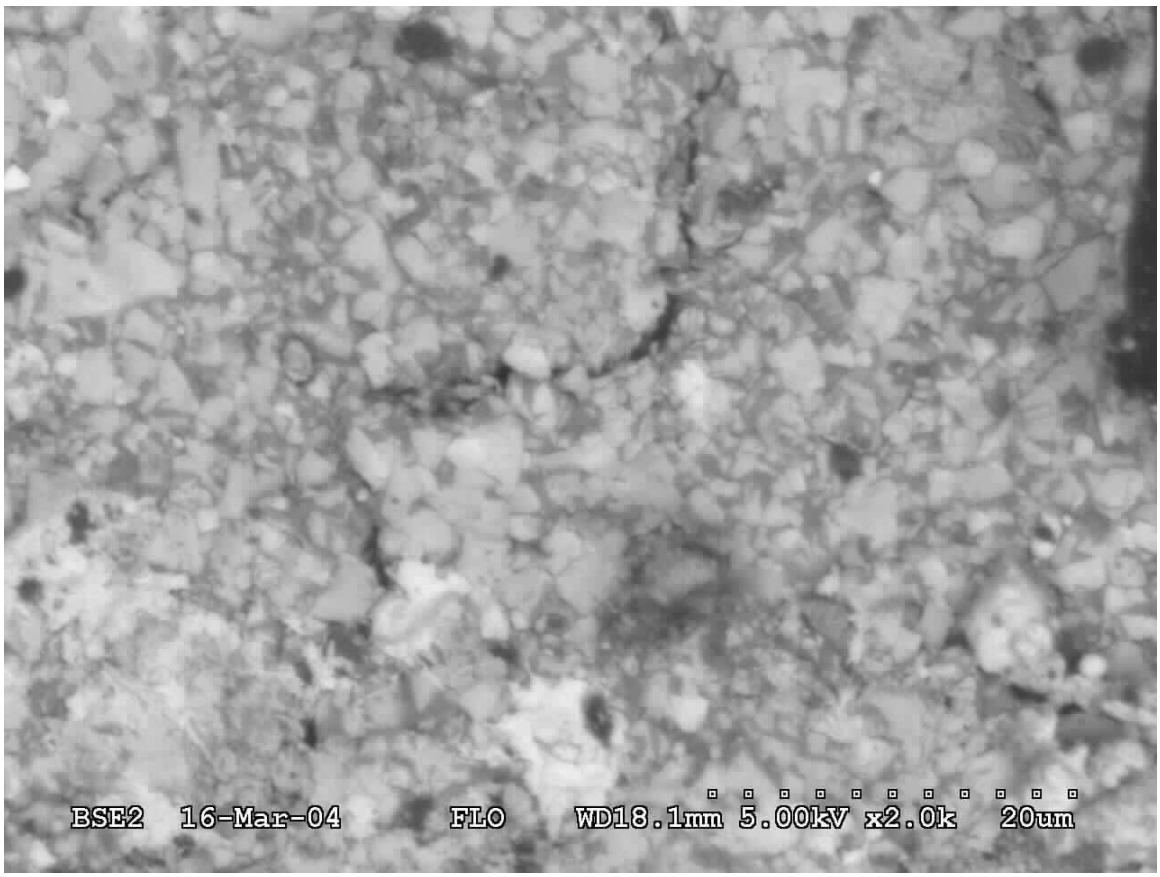

Figure 6.3: Backscatter of the same area as in fig. 6.3. (LOT …-00)

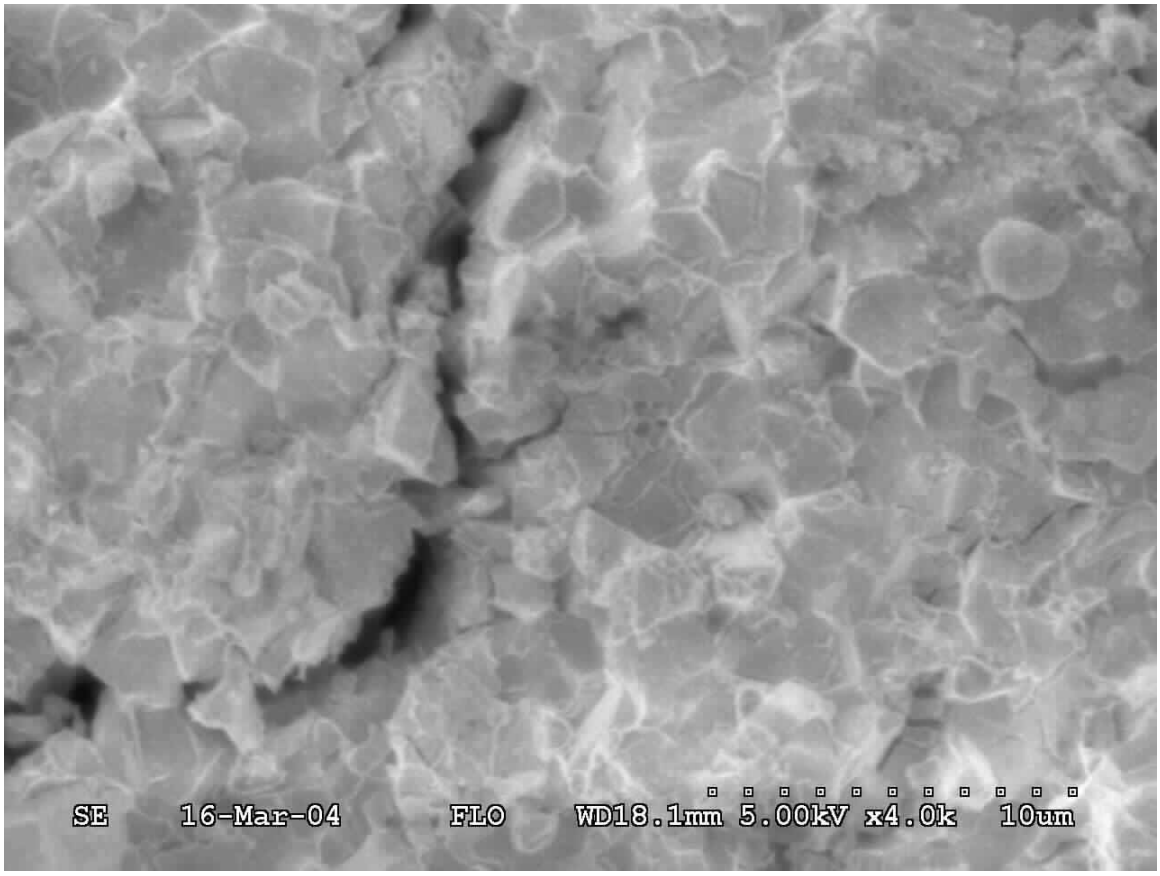

Figure 6.4: Fracture surface with crack. (LOT …-00)

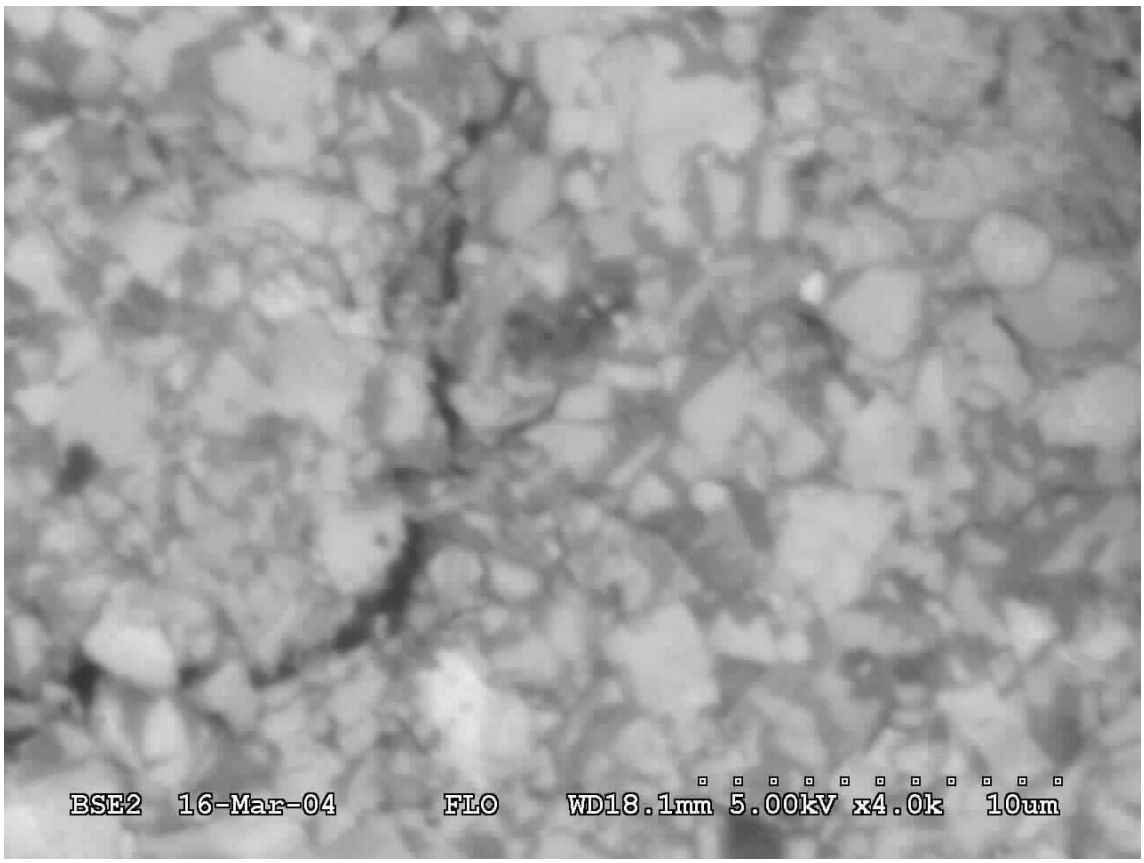

Figure 6.5: Backscatter of the same area as in fig. 6.4. (LOT …-00)

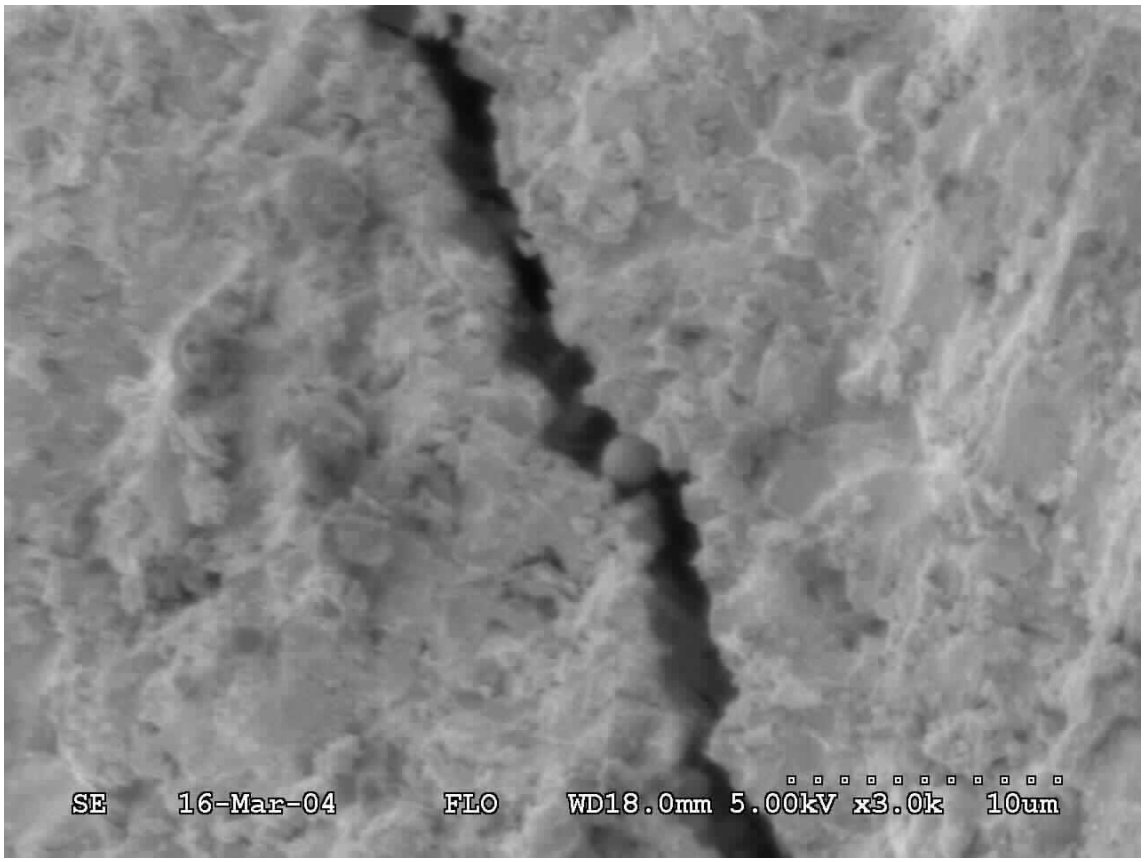

Figure 6.6: Fracture surface with crack. (LOT …-00)

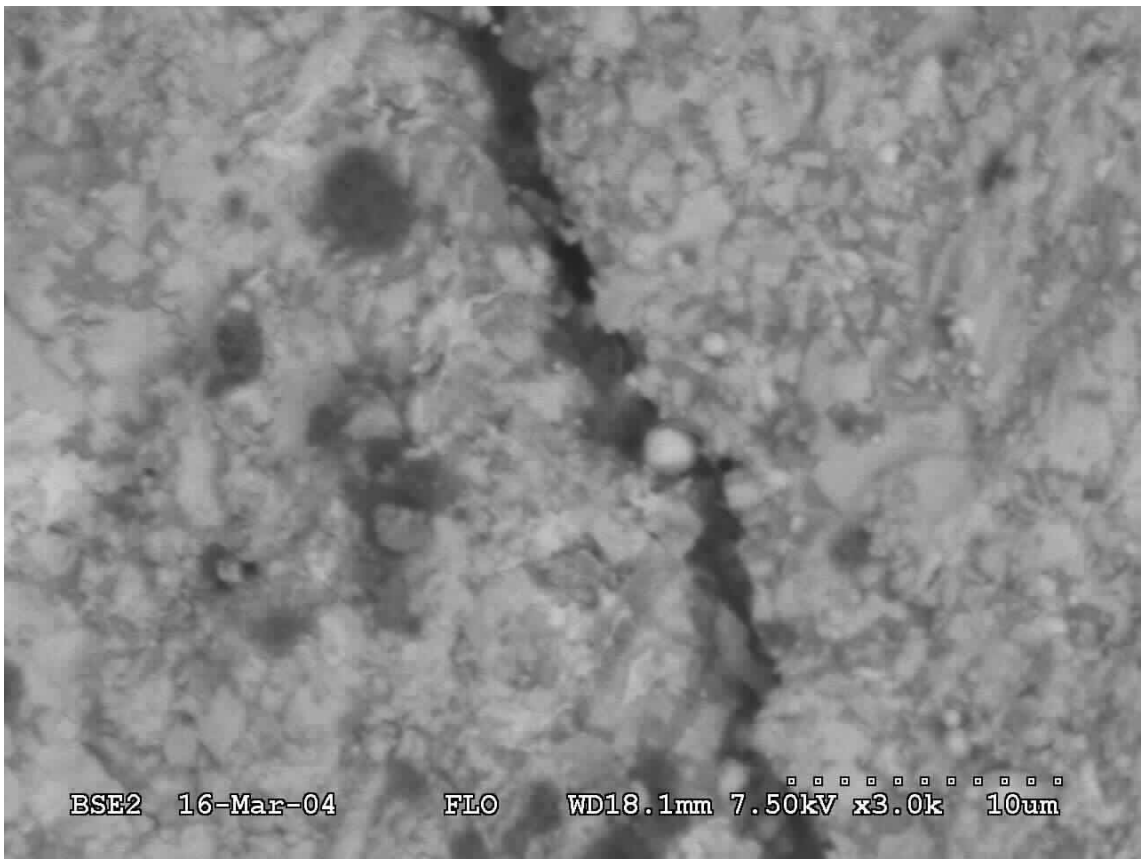

Figure 6.7: Backscatter of the same area as in fig. 6.6. (LOT …-00)

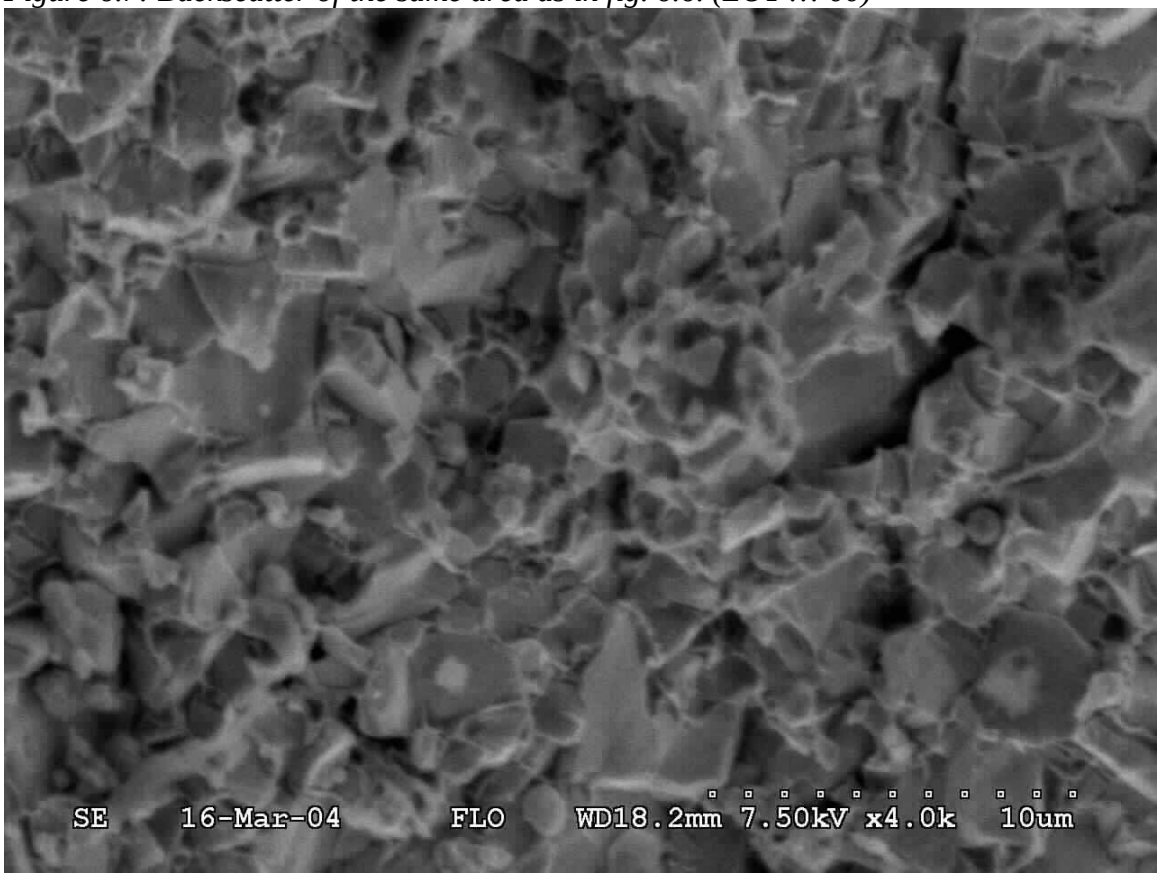

Figure 6.8: Microstructure of fracture surface. (LOT …-00)

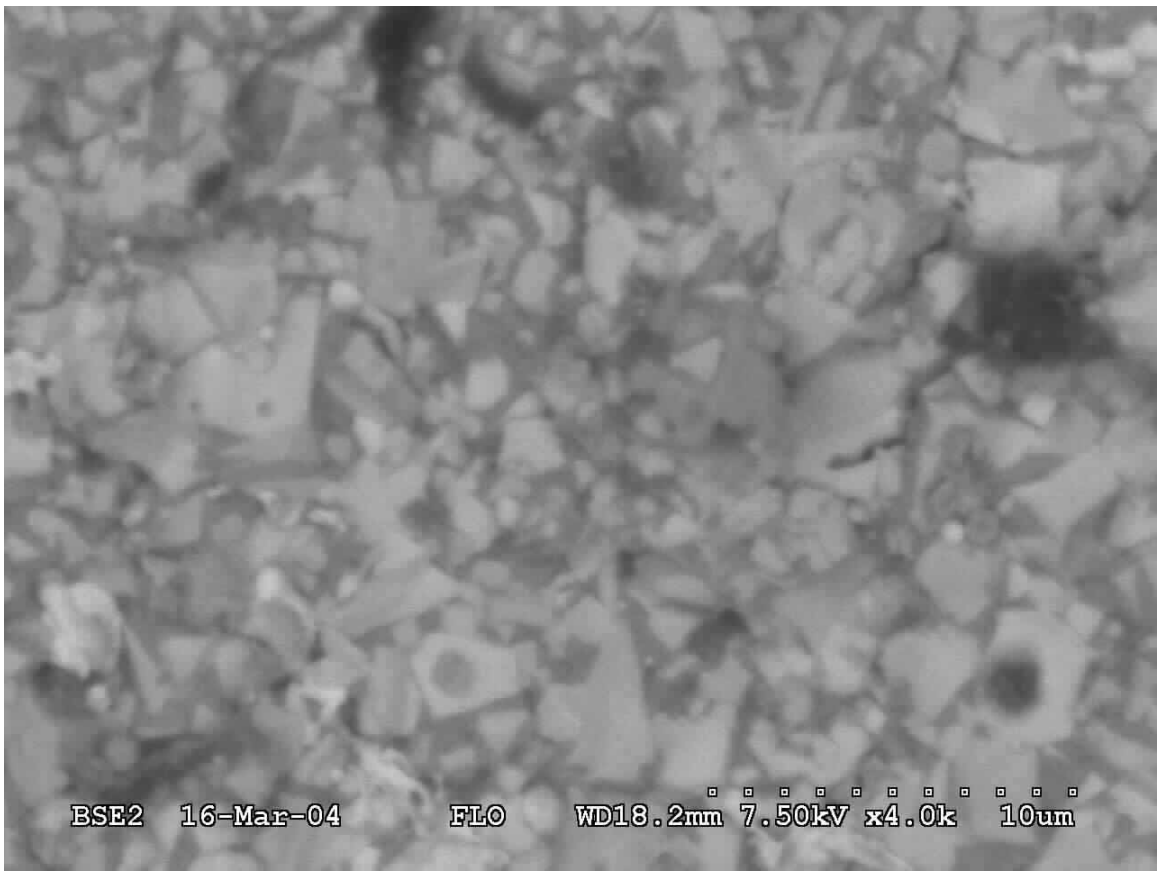

Figure 6.9: Backscatter of the same area as in fig. 6.8. (LOT …-00)

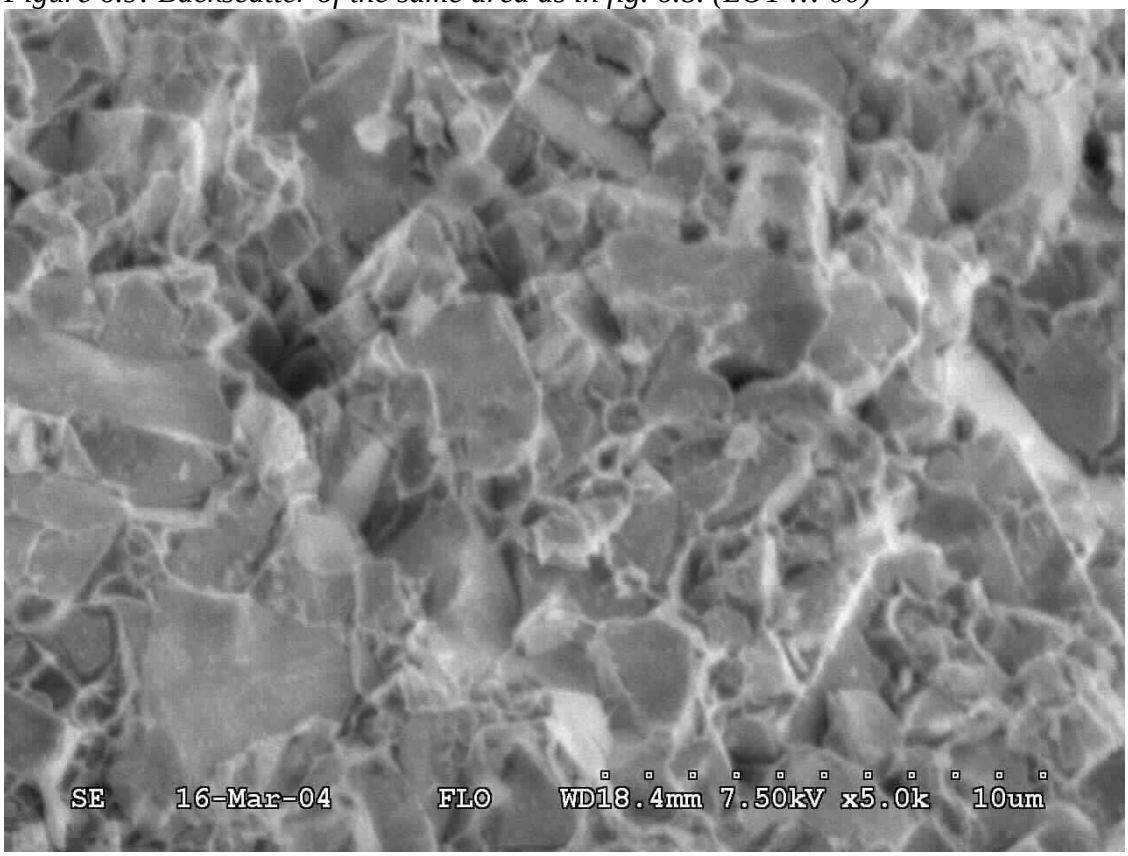

Figure 6.10: Microstructure of fracture surface. (LOT …-00)

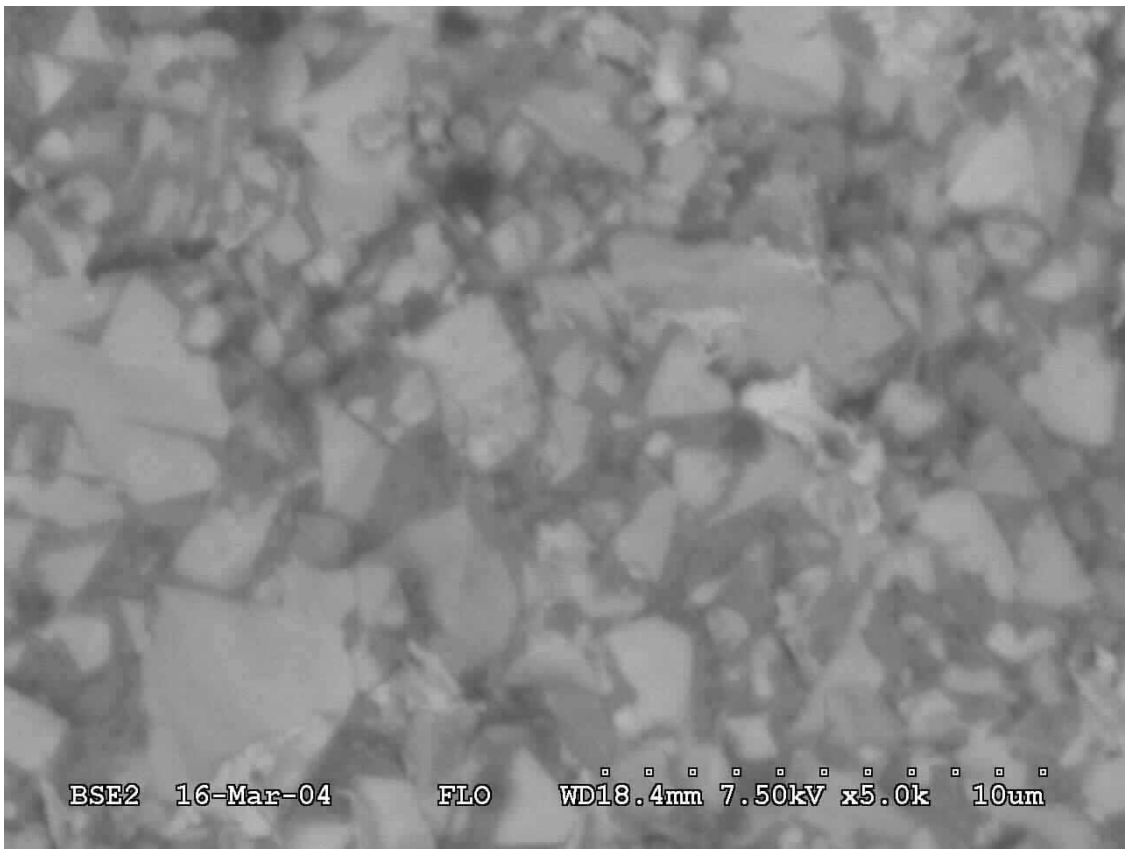

Figure 6.11: Backscatter of the same area as in fig. 6.10. (LOT …-00)

Also in this last case the fracture is intergranular because of the protruding geometric shape of the WC grains. The pictures however were not as clear this time because of the small size of the analysed specimen.

7 HARDNESS MEASUREMENT

Indentations into the WC-Co hardmetals with a Vickers and Rockwell hardness tester were made. WC-Co hardmetals from two different manufacturers were tested; Sandvik Hard Materials and Kennametal Hertel. The indenters that were used was a Vickers diamond and a Rockwell diamond. The Vickers diamond has the shape of a pyramid and the Rockwell diamond is conical. The hardness tests were made primarily to provoke cracks in the WC-Co hardmetal.

The Vickers tests were conducted with loads of 1, 10 and 30 kg. The Rockwell tests were conducted with a minor load of 3 kg and a major load of 15, 30 and 45 kg, respectively HR15N, HR30N and HR45N hardness tests.
Cracks were observed for 30 kg with Vickers and in one instance for Rockwell with a major load of 45 kg (HR45N). The cracks observed in the Vickers indentations started in the corners. Data from all the hardness measurements are presented in the appendix section.
From the pictures below we see that the cracks propagates mainly intergranular, but in some cases the crack goes transgranular (fig. 7.6 and 7.7).

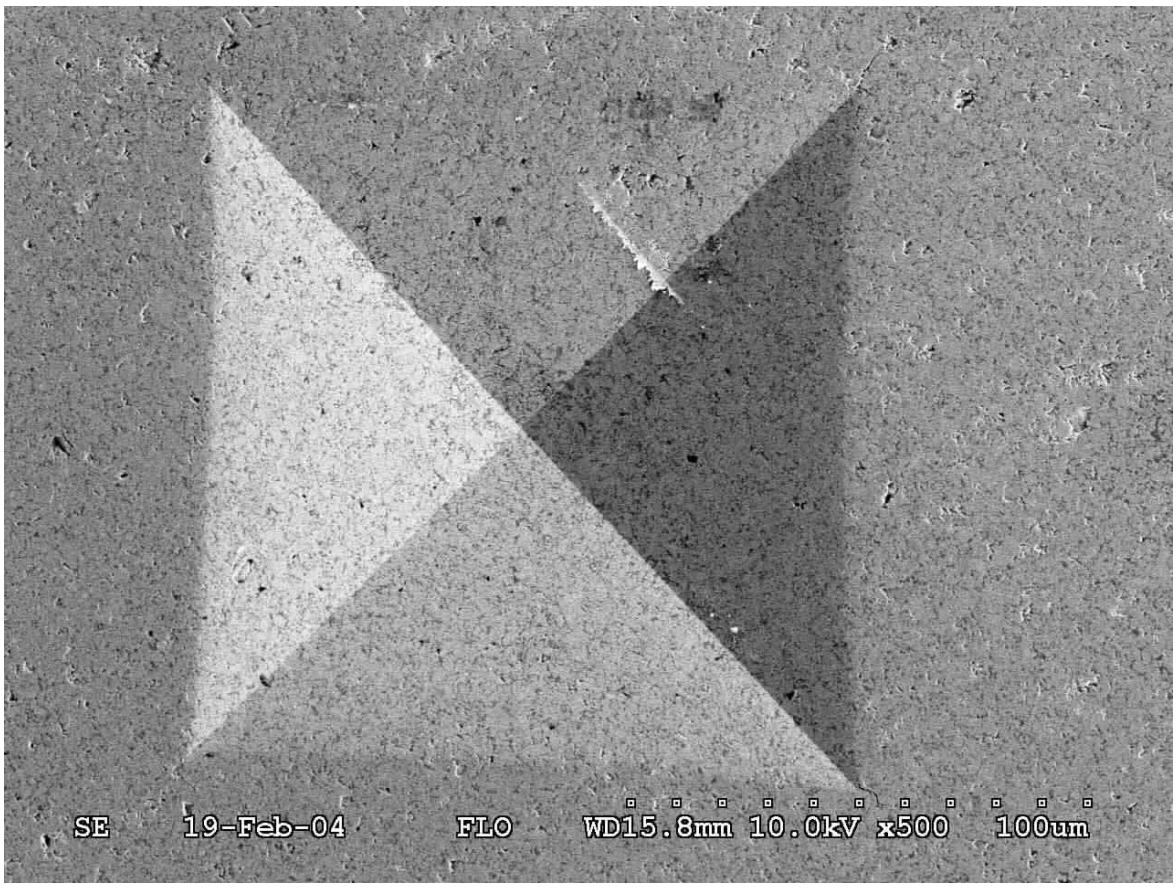

Figure 7.1: Hertel, Vickers indentation at 30 kg load, crack in upper and lower right corner.

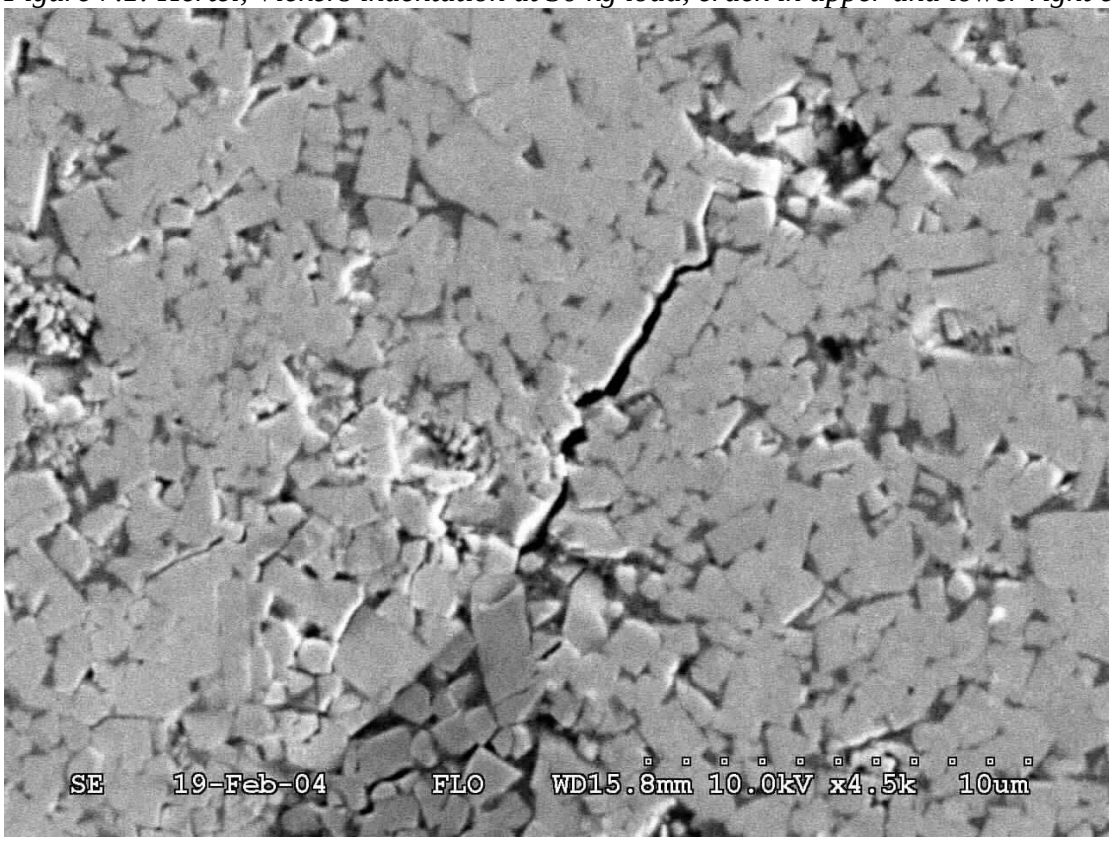

Figure 7.2: Close-up of the crack in the upper right corner from fig. 7.1.

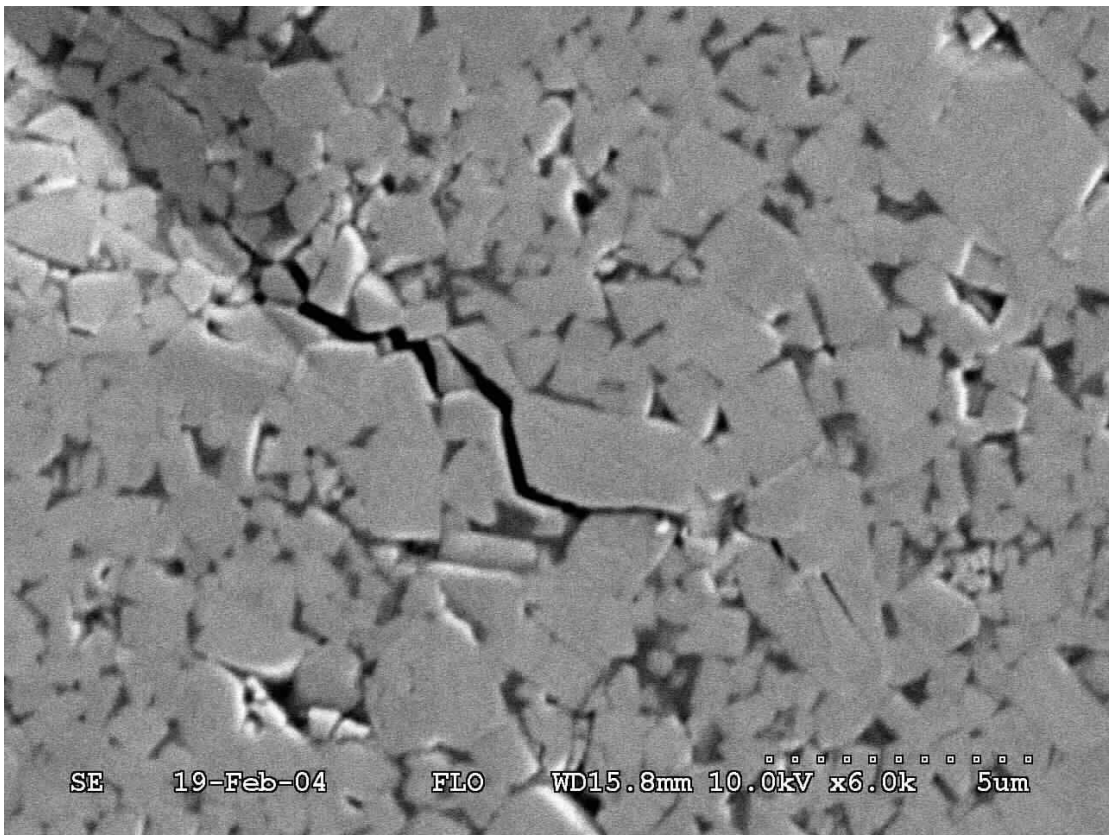

Figure 7.3: Close-up of the crack in the lower right corner from fig. 7.1.

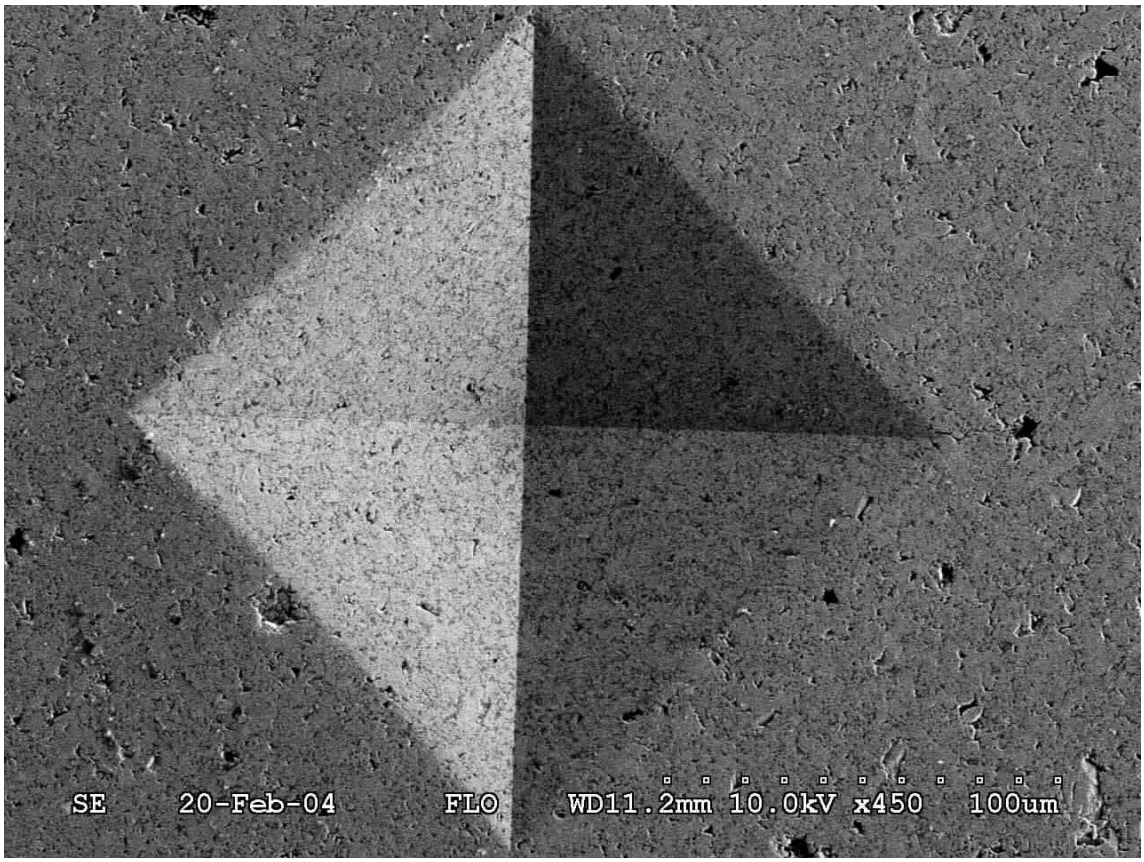

Figure 7.4: Sandvik, Vickers indentation at 30 kg load, crack in upper and right corner.

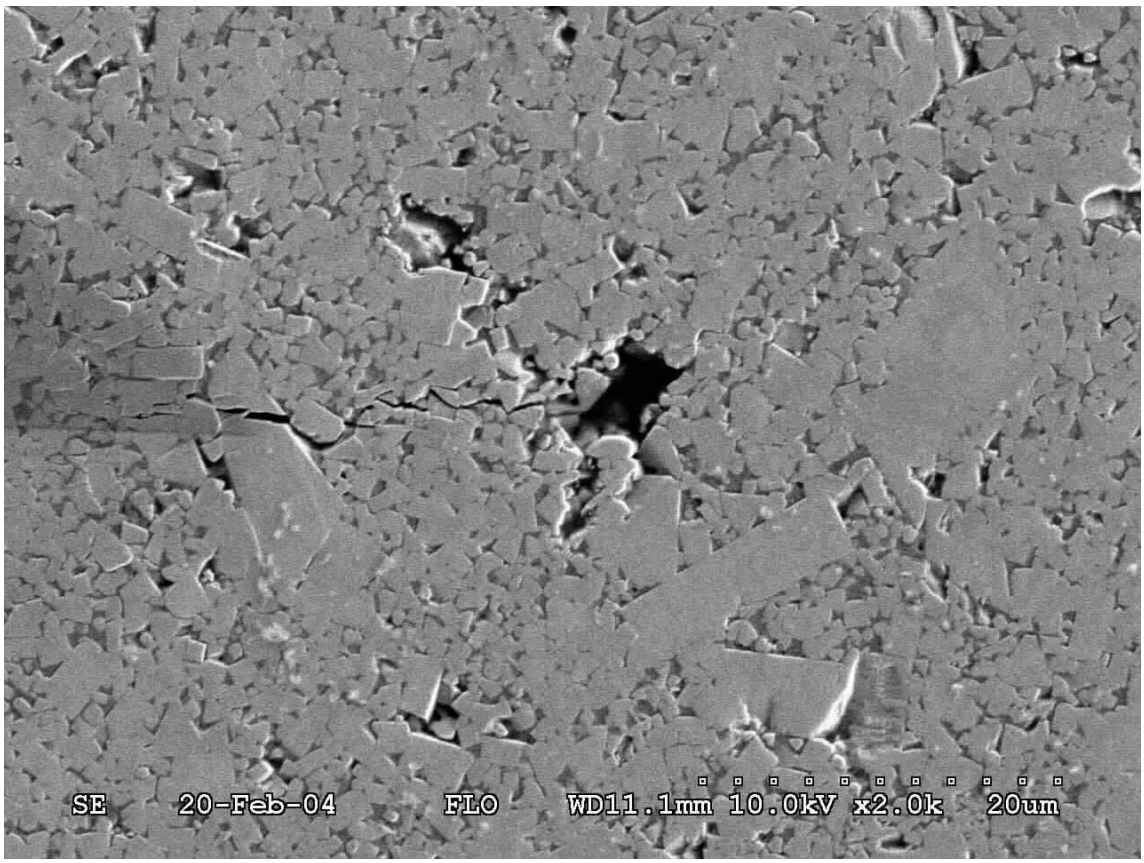

Figure 7.5: The crack in the right corner of fig. 7.4.

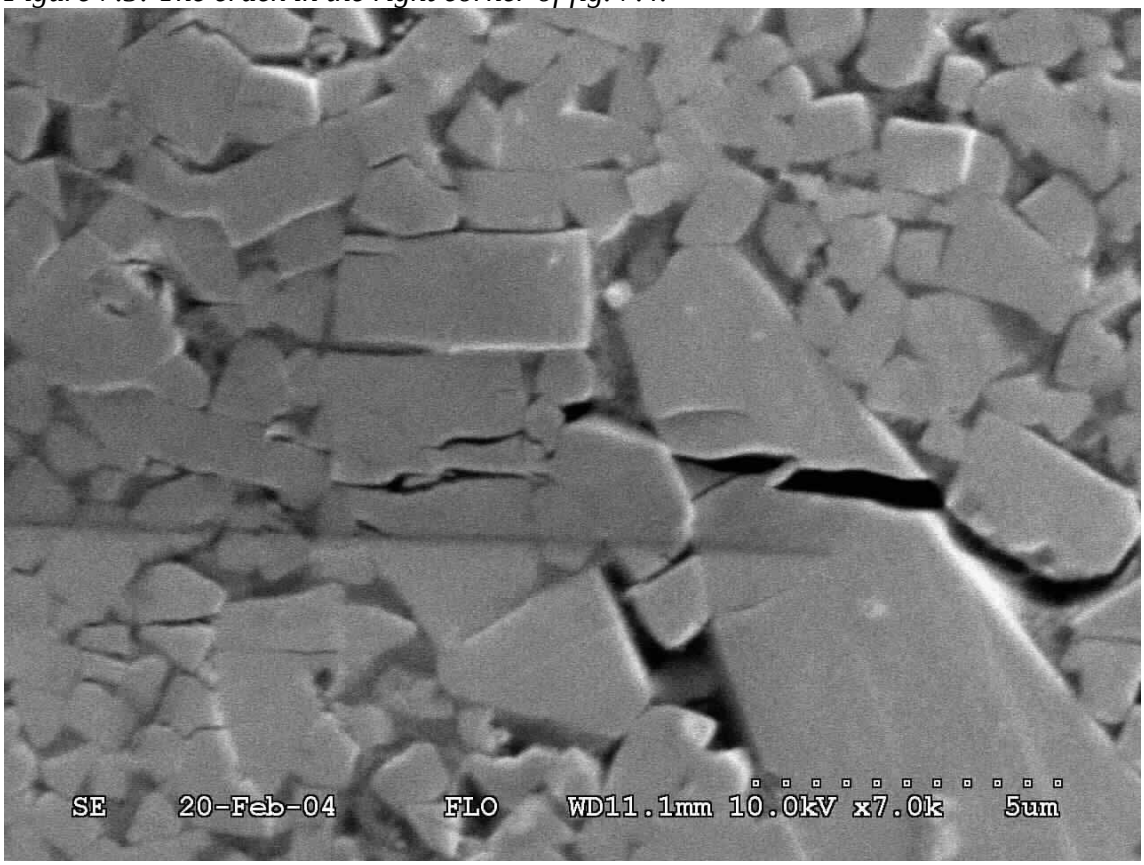

Figure 7.6: Close-up of the same crack as in fig. 7.5.

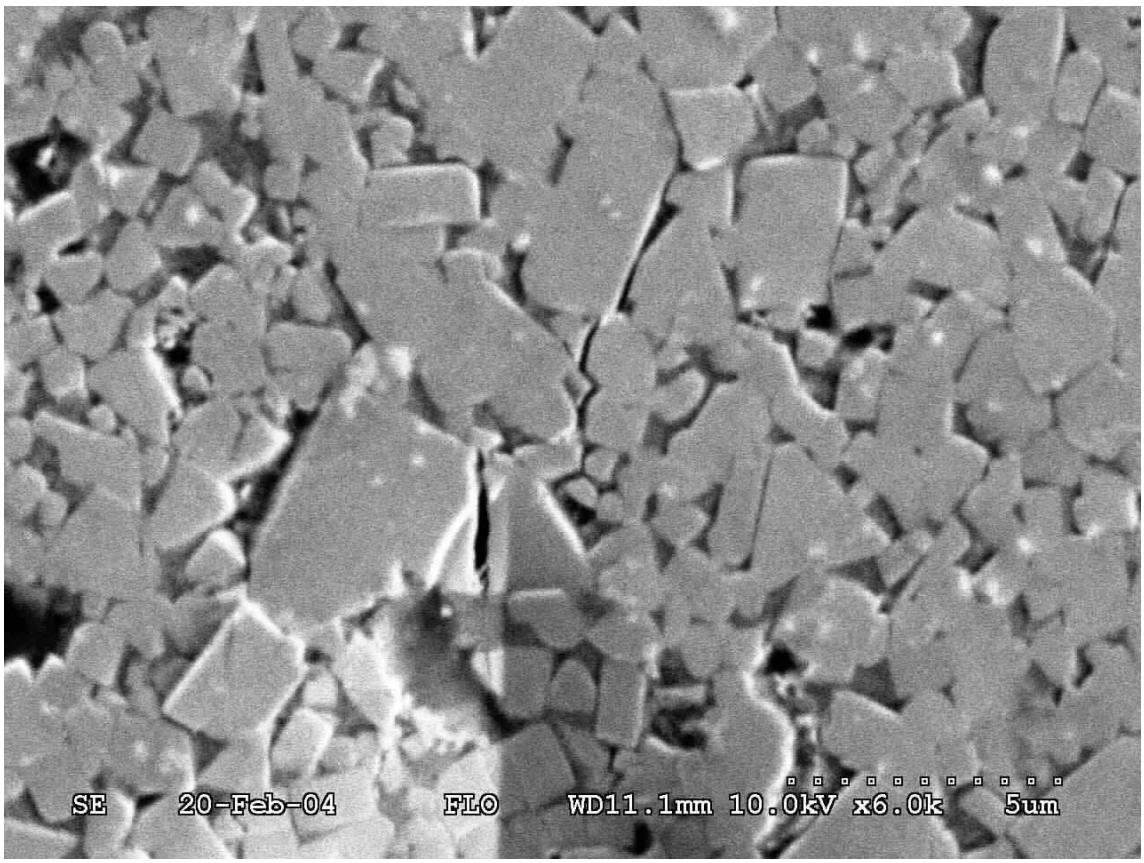

Figure 7.7: The crack in the upper corner of fig. 7.4.

Figure 7.8: Hertel, Rockwell at 45 kg major load, crack emanating from the lower right edge.

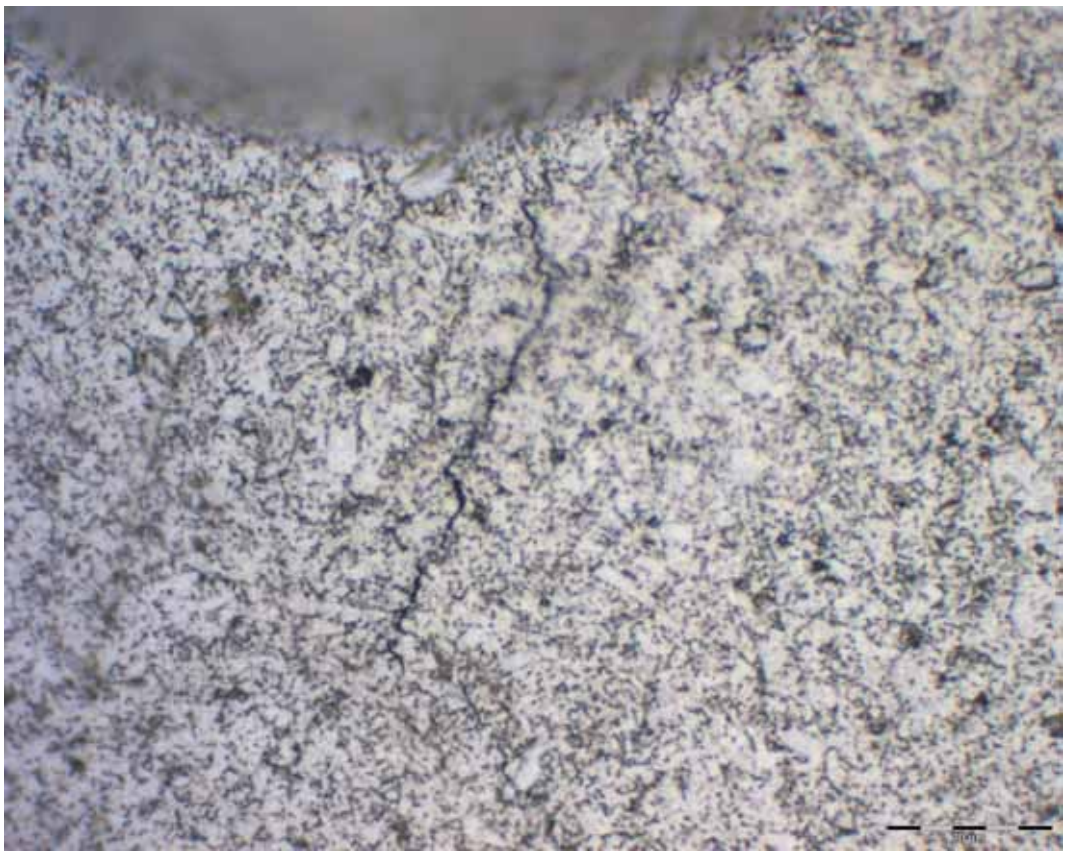

Figure 7.9: Close-up of the crack as shown in fig. 7.8.

8 "FINGER PRINTS" PARAMETERS

It is often desirable to interpret the mechanical behaviour in terms of structural features observed under the microscope. Our first parameter is the density given by the relation

$$1/\rho = \alpha_{Co}/\rho_{Co} + \alpha_{WC}/\rho_{WC} \tag{8.1}$$

where alpha gives the mass fraction of the different ingredients. Using that α_{Co}=0.099 and α_{WC}=0.901, ρ_{WC} = 15.65 10^3 kg/m^3, ρ_{CO} = 8.9 10^3 kg/m^3 gives that ρ = 14.55 10^3 kg/m^3. The density of the hardcore is reported to be (14.55 +/- 0.15) 10^3 kg/m^3. Thus the void fraction can be neglected. The spread in the experimental results for the density is probably related to scattering in the void fraction. The corresponding volume fractions are given by

$$V_{Co} = \frac{\alpha_{Co}/\rho_{Co}}{\alpha_{Co}/\rho_{Co} + \alpha_{WC}/\rho_{WC}} = \frac{\alpha_{Co}\rho}{\rho_{Co}} = 0.16, V_{WC} = \frac{\alpha_{WC}/\rho_{WC}}{\alpha_{Co}/\rho_{Co} + \alpha_{WC}/\rho_{WC}} = 0.84 \tag{8.2}$$

The particle size is given as (line intersection of sample cross section)

Kennametal Hertel (G15)
Average grain diameter d= 2.0 µm, standard deviation: 0.71 µm
for 31 random WC particles.

Sandvik Hard Material (H10N)
Average grain diameter d=2.6 µm, standard deviation: 1.83 µm
for 31 random WC particles.

The particle size can be calculated according to an experimental relation given by

$$d = 0.310^{-6} m \left(\frac{80kA/m}{H_c} \right)^{0.57/V_{Co}^{1/3}} \tag{8.3}$$

where H_c is an electric current pr meter (the coercive force). The experimental values gives H_c = 136 Ørstedt= 10.85 kA/m. Inserting into relation (8.3) gives that d= 2.44 10^{-6} m. Thus in good agreement with the line intercepts method.

Let us define the following variables

- C_{WC} = contact area sheared between WC grains/(contact area sheared between WC grains plus contact area sheared between WC grains and Cobalt)
- N_{WC} =number of interfaces WC-WC grains intercepted by a random line pr unit length.
- N_{WC-Co} = number of interfaces between WC and Co intercepted by a random line pr unit length.
- λ_{WC} = “free “ path in a WC phase
- λ_{Co} = “free” path in Co phase
- N_{WC}^{l} = number of WC grains intercepted pr unit length of a random line
- N_{WC}^{a} = number of WC grains intercepted pr unit area of a random cross section
- N_{WC}^{v} =number of WC grains pr unit volume of a random volume
- N_{WC}^{cv} =number of contacts between WC grains pr unit volume of a random volume
- N_{WC}^{c} = number of contacts between WC-WC grains pr grain
- a^c = sheared area by two WC grains in contact

If all WC grains are in contact throughout the complete surface it follows that $C_{WC} = 1$.
It can be shown that the contiguity, C_{WC}, can be calculated by the relation

$$C_{WC} = \frac{2N_{WC}}{2N_{WC} + N_{WC-Co}} \tag{8.4}$$

Furthermore the free path in WC can be calculated as

$$\lambda_{WC} = \frac{2V_{WC}}{N_{WC-Co}} \tag{8.5}$$

The average free path in the Cobalt is given by

$$\lambda_{Co} = d\frac{V_{Co}}{1-V_{Co}} = 0.46\,10^{-6} m \tag{8.6}$$

It also follows that

$$N_{WC}^{c} = \frac{2N_{WC}^{cv}}{N_{WC}^{v}} \tag{8.7}$$

$$a^{c} = C_{WC} / N_{WC}^{c} \tag{8.8}$$

By assuming identical spheres as a special case it follows that

$$\begin{aligned} &N_{WC}^{v} = \frac{\pi}{4} {N_{WC}^{a}}^{2} / N_{WC}^{l}, (a), N_{WC}^{cv} = \frac{2}{\pi} {N_{WC}^{a}}^{2} / N_{WC}, (b), \\ &\lambda_{WC} = \frac{\left(1-(a^{c})^{2} N_{WC}^{c}\right)\left(\frac{2}{3}d\right)}{1-a^{c} N_{WC}^{c}}, (c), a^{c} = \frac{1-Cos\left(\theta/2\right)}{3-Cos\left(\theta/2\right)}, (d), \\ &N_{WC}^{v} = \frac{\rho}{\frac{4}{3}\pi R^{3}\rho_{WC}}, (e), R = d/2, (f) \end{aligned} \tag{8.9}$$

where θ is the angle of two WC interphase boundaries at their junction with grain boundary. The following algorithm can be used with carefulness

- Measure N_{WC} and N_{WC-Co}
- Calculate C_{WC} according to (8.4)
- Calculate N_{WC}^{v} (8.9e)
- Measure N_{WC}^{a}
- Calculate N_{WC}^{l} (8.9a)
- Calculate N_{WC}^{c} and N_{WC}^{cv} by using (8.9b) and (8.7)
- Calculate a^{c} according to (8.8)
- Calculate λ_{WC} according to (8.5)

Further a relation gives the fracture toughness empirically as

$$K_{1c} = 8.75\,MPa\,m^{-1/2} + 10.83\,MPa\,m^{-1/2}\mu m^{-1}\lambda_{Co} \tag{8.10}$$

9 CONCLUSION/DISCUSSION

Our analysis indicates that the crack growth is similar in all cases. Some of the cracks seen in the hardness tests are clearly transgranular, but in most cases the crack will propagate intergranular. A more exact crack analysis by hardness testing will be done later. Although our analyses suggest that intergranular cracks are the most common case. This means that the strength could possible be increased by decreasing the WC particle size, or by increasing the amount of Cobalt.

Acknowledgements
Many thanks to Dr. Øyvind Frigaard at Forsvarets laboratorietjeneste for taking the SEM images.

References

[1] R. Morrell, Fractography of brittle materials, Measurement Good Practice Guide No. 15, National Physical Laboratory, 1999

[2] Bishop R.F., Hill R., Mott N.F., The Theory of Indentation and Hardness Tests, Proc.Phys.Soc.Vol.57, Part3, No.321, pp.147-159, May 1945

APPENDIX A

Data tables for the hardness tests of Kennametal Hertel and Sandvik WC-Co hardmetals

Hertel

Indenter type	Force [N]	Projected area [µm^2]	Force/area [GPa]	Cracks length [µm] Crack no. 1	Cracks length [µm] Crack no. 2
Pyramid (136°)	9.81	666	14.7	-	-
Pyramid	9.81	648	15.1	-	-
Pyramid	9.81	612	16.0	-	-
Pyramid	9.81	648	15.1	-	-
Pyramid	9.81	612	16.0	-	-
Pyramid	9.81	630	15.6	-	-
Pyramid	9.81	648	15.1	-	-
Pyramid	9.81	630	15.6	-	-
Pyramid	9.81	612	16.0	-	-
Pyramid	9.81	612	16.0	-	-
Pyramid	98.1	6670	14.7	-	-
Pyramid	98.1	6903	14.2	-	-
Pyramid	98.1	6728	14.6	-	-
Pyramid	294.3	21841	13.5	10	14
Conical (120°)	147.2	10899	13.5	-	-
Conical	147.2	10641	13.8	-	-
Conical	147.2	10532	14.0	-	-
Conical	147.2	10641	13.8	-	-
Conical	147.2	10477	14.0	-	-
Conical	294.3	18651	15.8	-	-
Conical	294.3	19310	15.2	-	-
Conical	294.3	19236	15.3	-	-
Conical	294.3	19483	15.1	-	-
Conical	294.3	19656	15.0	-	-
Conical	441.5	27759	15.9	-	-
Conical	441.5	27877	15.8	-	-
Conical	441.5	27671	16.0	-	-
Conical	441.5	27877	15.8	17	38 +
Conical	441.5	28055	15.7	-	-

Hertel

Indenter type	Force [N]	Average Force/area [GPa]	Std. deviation Force/area [GPa]
Pyramid	9.81	15.5	0.5
Pyramid	98.1	14.5	0.3
Conical	147.2	13.8	0.2
Conical	294.3	15.3	0.3
Conical	441.5	15.9	0.1

Sandvik						
					Cracks length [µm]	
Indenter type	Force [N]	Projected area [µm^2]	Force/area [GPa]		Crack no. 1	Crack no. 2
Pyramid (136°)	9.81	612	16.0		-	-
Pyramid	9.81	666	14.7		-	-
Pyramid	9.81	648	15.1		-	-
Pyramid	9.81	684	14.3		-	-
Pyramid	9.81	648	15.1		-	-
Pyramid	9.81	666	14.7		-	-
Pyramid	9.81	648	15.1		-	-
Pyramid	9.81	648	15.1		-	-
Pyramid	9.81	648	15.1		-	-
Pyramid	9.81	666	14.7		-	-
Pyramid	98.1	7140	13.7		-	-
Pyramid	98.1	7021	14.0		-	-
Pyramid	98.1	7565	13.0		-	-
Pyramid	294.3	21321	13.8		24	6
Conical (120°)	147.2	10532	14.0		-	-
Conical	147.2	11029	13.3		-	-
Conical	147.2	10405	14.1		-	-
Conical	147.2	11291	13.0		-	-
Conical	147.2	10899	13.5		-	-
Conical	294.3	20358	14.5		-	-
Conical	294.3	20867	14.1		-	-
Conical	294.3	20358	14.5		-	-
Conical	294.3	20867	14.1		-	-
Conical	294.3	20358	14.5		-	-
Conical	441.5	29498	15.0		-	-
Conical	441.5	29498	15.0		-	-
Conical	441.5	29712	14.9		-	-
Conical	441.5	29926	14.8		-	-
Conical	441.5	29712	14.9		-	-

Sandvik			
Indenter type	Force [N]	Average Force/area [GPa]	Std. deviation Force/area [GPa]
Pyramid	9.81	15.0	0.4
Pyramid	98.1	13.6	0.5
Conical	147.2	13.6	0.2
Conical	294.3	14.3	0.2
Conical	441.5	14.9	0.1